A rescaling-invariant Lipschitz bound based on path-metrics for modern ReLU network parameterizations

Antoine Gonon, Nicolas Brisebarre, Elisa Riccietti, Rémi Gribonval

A rescaling-invariant Lipschitz bound based on path-metrics for modern ReLU network parameterizations

Antoine Gonon[*], Nicolas Brisebarre[†], Elisa Riccietti[*], Rémi Gribonval[‡]

Abstract

Lipschitz bounds on neural network parameterizations are important to establish generalization, quantization or pruning guarantees, as they control the robustness of the network with respect to parameter changes. Yet, there are few Lipschitz bounds *with respect to parameters* in the literature, and existing ones only apply to simple feedforward architectures, while also failing to capture the intrinsic rescaling-symmetries of ReLU networks. This paper proves a new Lipschitz bound in terms of the so-called path-metrics of the parameters. Since this bound is intrinsically invariant with respect to the rescaling symmetries of the networks, it sharpens previously known Lipschitz bounds. It is also, to the best of our knowledge, the first bound of its kind that is broadly applicable to modern networks such as ResNets, VGGs, U-nets, and many more.

1 Introduction

An important challenge about neural networks is to upper bound as tightly as possible the distances between the so-called realizations (*i.e.*, the functions implemented by the considered network) $R_\theta, R_{\theta'}$ with parameters θ, θ' when evaluated at an input vector x, in terms of a (pseudo-)distance $d(\theta, \theta')$ and a constant C_x:

$$\|R_\theta(x) - R_{\theta'}(x)\|_1 \leqslant C_x d(\theta, \theta'). \tag{1}$$

This controls the robustness of the function R_θ with respect to changes in the parameters θ, which can be crucially leveraged to derive generalization bounds [Neyshabur et al., 2018] or theoretical guarantees about pruning or quantization algorithms [Gonon et al., 2023]. Yet, to the best of our knowledge, the literature is very terse on such bounds, and existing ones are expressed with ℓ^p metrics on parameters [Berner et al., 2020, Gonon et al., 2023, Neyshabur et al., 2018]. For example, such a bound is known [Gonon et al., 2023, Theorem III.1 with $p = \infty$ and $q = 1$] with

$$d(\theta, \theta') := \|\theta - \theta'\|_\infty, \qquad C_x := (W\|x\|_\infty + 1)WL^2R^{L-1}, \tag{2}$$

in the case of a layered fully-connected neural network $R_\theta(x) = M_L \,\mathrm{ReLU}(M_{L-1} \dots \mathrm{ReLU}(M_1 x))$ with L layers, maximal width W, and with weight matrices M_ℓ having some operator norm bounded by R. Moreover, these known bounds are not satisfying for at least two reasons:

- they are **not invariant under neuron-wise rescalings** of the parameters θ that leave unchanged its realization R_θ. As we will show, this implies that numerical evaluations of such bounds can be arbitrarily large;
- they **only hold for simple fully-connected models organized in layers**, but not for modern networks that include pooling, skip connections, etc.

To circumvent these issues, this work proposes to leverage the so-called *path-lifting*, a tool that has recently emerged [Bona-Pellissier et al., 2022, Gonon et al., 2024, Marcotte et al., 2023, Stock and Gribonval, 2023] in the theoretical analysis of modern neural networks with positively homogeneous activations.

[*]ENS de Lyon, CNRS, Université Claude Bernard Lyon 1, Inria, LIP, UMR 5668, 69342, Lyon cedex 07, France.
[†]CNRS, ENS de Lyon, Université Claude Bernard Lyon 1, Inria, LIP, UMR 5668, 69342, Lyon cedex 07, France
[‡]Inria, ENS de Lyon, CNRS, Université Claude Bernard Lyon 1, LIP, UMR 5668, 69342, Lyon cedex 07, France

Main contribution. This work introduces a natural (rescaling-invariant) *metric* based on the *path-lifting*, and shows that it indeed yields a *rescaling-invariant upper bound for the distance of two realizations of a network*. Specifically, denoting $\Phi(\theta)$ the path-lifting (a finite-dimensional vector whose definition will be recalled in Section 2) of the network parameters θ, we establish (Theorem 3.1) that for any input x, and network parameters θ, θ' *with the same coordinatewise signs*:

$$\|R_\theta(x) - R_{\theta'}(x)\|_1 \leqslant \max\left(\|x\|_\infty, 1\right) \|\Phi(\theta) - \Phi(\theta')\|_1. \tag{3}$$

We call $d(\theta, \theta') := \|\Phi(\theta) - \Phi(\theta')\|_1$ the ℓ^1*-path-metric*, by analogy with the so-called ℓ^1*-path-norm* $\|\Phi(\theta)\|_1$, see *e.g.* Barron and Klusowski [2019], Gonon et al. [2024], Neyshabur et al. [2015]. Of course, since the ℓ^1-norm is the largest ℓ^q-norm ($q \geqslant 1$), this also implies the same inequality for any ℓ^q-norm on the left-hand side. Besides being intrinsically rescaling-invariant, Inequality (3) holds for the very same general neural network model as in Gonon et al. [2024] that encompasses pooling, skip connections and so on. This solves the two problems mentioned above and improves on Equation (2). Finally, we show that, under conditions that hold in practical pruning and quantization scenarios, the path-metric is easy to compute in two forward passes, and we provide the corresponding `pytorch` implementation.

Our main theoretical finding, Inequality (3), together with the known properties of Φ [Gonon et al., 2024] confirms that the path-lifting Φ provides an intermediate space between the parameter space and the function space, that shares some advantages of both, see Table 1.

Table 1: The path-lifting provides an intermediate space between parameters and function spaces.

	 parameters space	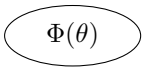 path-lifting space	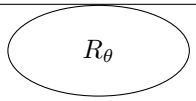 function space
	what we end up analyzing	**what we should analyze?**	what we want to analyze
dim$< \infty$	✓	✓	✗
invariance	✗	✓	✓
relation to R_θ	locally polynomial	locally linear	

Plan. The theoretical model we consider builds upon the framework introduced in Gonon et al. [2024], designed to encapsulate standard components of modern neural networks such as ReLU activations, max-pooling, and skip connections. A key motivation for our work is to develop Lipschitz bounds that remain invariant under rescaling. To achieve this, we recall the concept of path-lifting and introduce the main tools needed for our analysis (explained in Section 2).

Our main contribution is a rescaling-invariant Lipschitz bound on the distance between functions parameterized differently, expressed through the ℓ^1-path-metric. We discuss how it improves over existing bounds, how it can be computed, and why it matters for understanding neural networks in Section 3 (Theorem 3.1, establishing Inequality (3)).

We then look at how this bound can be applied to pruning by guiding which parameters can be safely removed while preserving accuracy. This application underscores the practical significance of our theoretical contribution, opening opportunities for more efficient model compression (Section 4).

2 ReLU DAGs, invariances, and path-lifting

The neural network model we consider generalizes and unifies several models from the literature, including those from Bona-Pellissier et al. [2022], DeVore et al. [2021], Kawaguchi et al. [2017], Neyshabur et al. [2015], Stock and Gribonval [2023], as detailed in Gonon et al. [2024, Definition 2.2]. This model allows for any Directed Acyclic Graph (DAG) structure incorporating standard features[1] such as max-pooling, average-pooling, skip connections, convolutional layers, and batch normalization layers, thus covering modern networks like ResNets, VGGs, AlexNet, etc. The full and formal definition of the model is in Appendix A.

[1]With the exception of the attention mechanism.

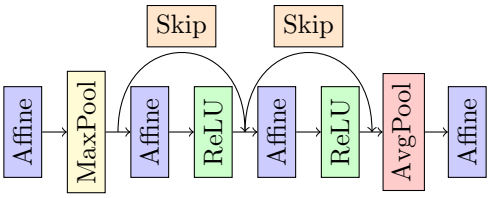

Figure 1: A network with the same ingredients as a ResNet.

2.1 Rescaling symmetries.

All network parameters (weights and biases) are gathered in a parameter vector θ, and we denote $R_\theta(x)$ the output of the network when evaluated at input x (the function $x \mapsto R_\theta(x)$ is the so-called *realization* of the network with parameters θ). Due to positive-homogeneity of the ReLU function $t \to \mathrm{ReLU}(t) := \max(0, t)$, in the simple case of a single neuron with no bias we have $R_\theta(x) = v \max(0, \langle u, x \rangle)$ with $\theta = (u, v)$, and for any $\lambda > 0$, the "rescaled" parameter $\tilde{\theta} = (\lambda u, \frac{v}{\lambda})$ implements the same function $R_{\tilde{\theta}} = R_\theta$. A similar rescaling-invariance property holds for the general model of Gonon [2024], Stock and Gribonval [2023] leading to the notion of rescaling-equivalent parameters, denoted $\tilde{\theta} \sim \theta$, which still satisfy $R_{\tilde{\theta}} = R_\theta$.

Need for rescaling-invariant Lipschitz bounds. Consider our initial problem of finding a pseudo-metric $d(\theta, \theta')$ and a constant C_x for any input x, for which (1) holds. The left hand-side of (1) is invariant under rescaling-symmetries: if $\tilde{\theta} \sim \theta$ then $\|R_{\tilde{\theta}}(x) - R_{\theta'}(x)\|_1 = \|R_\theta(x) - R_{\theta'}(x)\|_1$. However, when $d(\cdot, \cdot)$ is based on a standard ℓ^p norm, the right hand-side of (1) is *not* invariant, and in fact $\sup_{\tilde{\theta} \sim \theta} \|\tilde{\theta} - \theta'\|_p = +\infty$, so the bound can in fact be arbitrarily pessimistic:

$$\sup_{\tilde{\theta} \sim \theta} \frac{d(\tilde{\theta}, \theta')}{\|R_{\tilde{\theta}}(x) - R_{\theta'}(x)\|_1} = \infty.$$

Although in general one could *make a bound such as* (1) *invariant* by considering the infimum

$$\inf_{\tilde{\theta} \sim \theta, \tilde{\theta}' \sim \theta'} d(\tilde{\theta}, \tilde{\theta}'),$$

this infimum may be difficult to compute in practice. Therefore, a "good" bound should ideally be both invariant under rescaling symmetries and easy to compute. Invariance to rescaling symmetries is precisely the motivation for the introduction of the path-lifting.

2.2 Path-lifting Φ and path-activation matrix A.

For network parameters θ and input x, this paper considers the path-lifting vector $\Phi(\theta)$ and the path-activation matrix $A(\theta, x)$ as defined in Gonon et al. [2024, Definition A.1] for such general networks. We now give a simple description of these objects that will be sufficient to grasp the main results of this paper. The full definitions are recalled in Appendix A.

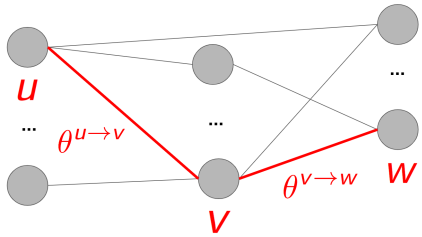

Figure 2: The coordinate of the path-lifting Φ associated with the path $p = u \to v \to w$ is $\Phi_p(\theta) = \theta^{u \to v} \theta^{v \to w}$.

The vector $\Phi(\theta) \in \mathbb{R}^{\mathcal{P}}$ is indexed by the set $\mathcal{P}$ of *paths* of the network (hence the name path-lifting), where a path is a sequence of connected nodes (neurons) starting at some neuron (an input neuron in the case

of networks without biases; in the presence of bias there are also paths starting from each hidden neuron) and ending at an output neuron. For instance, in the case of a simple one-hidden-layer ReLU network with no bias, $p = u \to v \to w$ is a path if u is an input neuron, v is a hidden neuron, and w is an output neuron. The coordinate of $\Phi(\theta)$ associated with a path is the product of the weights along this path, ignoring the non-linearities. For instance, if $\theta^{a\to b}$ denotes the weight of the edge $a \to b$, we have $\Phi_p(\theta) := \theta^{u\to v}\theta^{v\to w}$ for the path $p = u \to v \to w$, see Figure 2.

The information about non-linearities is stored in binary form ($\{0,1\}$) in the so-called *path-activation matrix*, which in the case of a network without bias is a matrix $A(\theta, x) \in \{0,1\}^{\mathcal{P}\times d_{\text{in}}}$ indexed by the paths p and the input coordinates $u \in [\![1, d_{\text{in}}]\!]$: $(A(\theta, x))_{p,u} := 1$ if and only if all neurons along path p are activated and p starts at the input neuron u.

In networks with biases, the definitions are similar, but the set of paths $\mathcal{P}$ also includes paths starting from hidden neurons. The matrix A is then indexed by an additional input coordinate to account for biases, resulting in $A(\theta, x) \in \{0,1\}^{\mathcal{P}\times(d_{\text{in}}+1)}$.

Key properties of (Φ, A). The essential properties are

- $\Phi(\theta)$ is a vector, whose entries are monomial functions of the coordinates of θ;
- $A(\theta, x)$ is a binary matrix, and is a piecewise constant function of (θ, x),
- both $\Phi(\theta)$ and $A(\theta, x)$ are rescaling-invariant: if $\tilde{\theta} \sim \theta$ then $\Phi(\tilde{\theta}) = \Phi(\theta)$ and $A(\tilde{\theta}, x) = A(\theta, x)$ for every x [Gonon, 2024, Theorem 2.4.1]
- the network output is a simple function of these two objects: for scalar-valued networks it holds

$$R_\theta(x) = \left\langle \Phi(\theta), A(\theta, x) \begin{pmatrix} x \\ 1 \end{pmatrix} \right\rangle \tag{4}$$

and a similar simple formula holds for vector-valued networks [Gonon et al., 2024, Theorem A.1].

Example: For a simple one-hidden-layer network without bias, with parameters $\theta = (u_1, \dots, u_k, v_1, \dots, v_k)$ with $u_i \in \mathbb{R}^{d_{\text{in}}}$, $v_i \in \mathbb{R}^{d_{\text{out}}}$ and associated function $R_\theta(x) = \sum_{i=1}^k \max(0, \langle x, u_i\rangle)v_i \in \mathbb{R}^{d_{\text{out}}}$, the path-lifting is simply given by $\Phi(\theta) = (u_i v_i^T)_{i\in[\![1,k]\!]} \in \mathbb{R}^{kd_{\text{in}}d_{\text{out}}}$. The path-activation matrix $A(\theta, x) \in \mathbb{R}^{kd_{\text{in}}d_{\text{out}}\times(d_{\text{in}}+1)}$ is simply $\mathbf{I}_{d_{\text{in}}} \otimes (\mathbb{1}_{\langle x,u_i\rangle>0})_{i\in[\![1,k]\!]} \otimes \mathbf{1}_{d_{\text{out}}}$, concatenated with $\mathbf{0}_{kd_{\text{in}}d_{\text{out}}}$ (zeros because there are no biases here). We denote by $\mathbf{I}_d$ the identity matrix of size $d \times d$ and $\mathbf{1}_d$ (resp. $\mathbf{0}_d$) the column vector of size d filled with ones (resp. zeros). On this simple example, it is easy to see that both $\Phi(\theta)$ and $A(\theta, x)$ are invariant under the neuron-wise rescaling $\theta \mapsto \lambda \diamond \theta$ corresponding to $(v_i, u_i) \to (\frac{1}{\lambda_i}v_i, \lambda_i u_i)$ with $\lambda \in (R_{>0})^k$, that leaves invariant the associated function: $R_\theta = R_{\lambda\diamond\theta}$ [Gonon et al., 2024].

Related work. The path-lifting, (together with its norm, called the *path-norm*), has already been used to derive guarantees of identifiability [Bona-Pellissier et al., 2022, Stock and Gribonval, 2023], characterizations of the training dynamics [Marcotte et al., 2023], Lipschitz bounds *with respect to the input* x for a given θ Gonon et al. [2024], and generalization bounds [Gonon et al., 2024, Neyshabur et al., 2015]. Its invariance under some rescaling symmetries of the network is nicely complemented by the ease of computation of the path-norm [Gonon et al., 2024]. While these tools have long been limited to simple network architectures [Bona-Pellissier et al., 2022, Kawaguchi et al., 2017, Neyshabur et al., 2015, Stock and Gribonval, 2023], they were recently extended [Gonon et al., 2024] to modern architectures by including most of their standard ingredients with the exception of attention mechanisms.

3 A rescaling invariant Lipschitz bound

Our main result, Theorem 3.1, is a Lipschitz bound with respect to the parameters of the network, as opposed to widespread Lipschitz bounds with respect to the inputs. It precisely proves that (1) holds with a rescaling-invariant pseudo-distance (called the ℓ^1-path metric) defined via Φ as $d(\theta, \theta') := \|\Phi(\theta) - \Phi(\theta')\|_1$ and $C_x = \max(\|x\|_\infty, 1)$.

Theorem 3.1. *Consider a ReLU DAG neural network, corresponding to an arbitrary DAG network with max-pool etc. as in Section 2, see Figure 1 for an illustration and Definition A.2 in the appendix for a precise definition. Consider parameters vectors θ, θ'. If for every coordinate i, $\theta_i\theta'_i \geqslant 0$, then for every input x:*

$$\|R_\theta(x) - R_{\theta'}(x)\|_1 \leqslant \max(\|x\|_\infty, 1)\|\Phi(\theta) - \Phi(\theta')\|_1. \tag{5}$$

Moreover, for every such neural network architecture, there are parameters $\theta \neq \theta'$ and an input x such that Inequality (5) is an equality.

Since $\|\cdot\|_q \leqslant \|\cdot\|_1$ for any $q \geqslant 1$, Inequality (5) implies the same bound with the ℓ^q-norm on the left hand-side.

We sketch the proof in Section 3.4. The complete proof is in Appendix B – we actually prove something slightly stronger, but we stick here to Inequality (5) for simplicity.

The Lipschitz bound (5) have several consequences. It can for example be used to derive so-called generalization bounds via the classical Dudley's integral [Bach, 2024, Shalev-Shwartz and Ben-David, 2014]. Specifically, consider the set of functions $\mathcal{F} := \{R_\theta, \|\Phi(\theta)\|_1 \leqslant r\} = \bigcup_{\text{signs } s} \{R_\theta, \|\Phi(\theta)\|_1 \leqslant r, \text{sgn}(\theta) = s\}$. The Rademacher complexity of $\mathcal{F}$ is a bound on the generalization error of any estimator taking values in $\mathcal{F}$, and Dudley's integral is itself a bound on this Rademacher complexity. Dudley's integral can in turn be bounded from above by bounds on the covering number of each set $\{R_\theta, \|\Phi(\theta)\|_1 \leqslant r, \text{sgn}(\theta) = s\}$ with prescribed signs. Inequality (5) precisely allows us to derive such covering bounds via covering numbers of the finite-dimensional sets $\{\Phi(\theta) : \text{sgn}(\theta) = s, \|\Phi(\theta)\|_1 \leqslant r\}$. The generalization bounds obtained directly in this way are however not as tight as those obtained by Gonon et al. [2024] based on the path-norm. Other consequences of the Lipschitz bound (5) can also be envisioned, and we will later explore its potential for pruning, see Section 4.

In the rest of this section, we discuss the assumptions of the theorem, the practical computation of the bound and the positioning with respect to previously established Lipschitz bounds.

3.1 Discussion on the sign assumption $(\theta_i \theta'_i \geqslant 0, \forall i)$.

The sign assumption in Theorem 3.1 is essential and cannot be simply relaxed (see Figure 5 in Appendix B). In practice, this sign assumption is naturally satisfied in many scenarios. Many interesting operations on θ are sign preserving: pruning, quantization, and even taking a small enough gradient step. Moreover, locally around any θ with no zero entry, there is a ball in which the signs are preserved. The size of this ball increases with the magnitude of the smallest entry in θ. Even in use cases where this sign assumption does not hold, Theorem 3.1 can serve as a building block for more general analyses. For example, as already evoked after Theorem 3.1, to establish generalization results in the full parameter space (without sign constraints), one can somehow "glue" together bounds established separately in each quadrant with fixed signs using Theorem 3.1.

3.2 Approximation and exact computation of ℓ^1-path-metrics

Since $\Phi(\theta)$ is a vector of combinatorial dimension (it is indexed by paths), it would be intractable to compute the ℓ^1-path metric $\|\Phi(\theta) - \Phi(\theta')\|_1$ by direct computation of the vector $\Phi(\theta) - \Phi(\theta')$. In this section we investigate efficient *and rescaling-invariant* approximations of the ℓ^1-path-metric that turn out to yield exact implementations in cases of practical interest.

A key fact on which the approach is built is that the ℓ^1-path-norm itself can be computed in one forward pass [Gonon et al., 2024]. Since, by the lower triangle inequality, we have

$$\Big| \|\Phi(\theta)\|_1 - \|\Phi(\theta')\|_1 \Big| \leqslant \|\Phi(\theta) - \Phi(\theta')\|_1, \tag{6}$$

the left-hand side of (6) serves as an approximation that can be computed in two forward passes of the network[2].

As we now show, this is not only completed by a rescaling-invariant upper bound (cf. Inequality (8) below), but is also an *exact evaluation* of the ℓ^1-path-metric under practical assumptions.

Lemma 3.2. *Inequality (6) is an equality as soon as $|\Phi(\theta)| \geqslant |\Phi(\theta')|$ coordinatewise: in this case we have*

$$\|\Phi(\theta) - \Phi(\theta')\|_1 = \|\Phi(\theta)\|_1 - \|\Phi(\theta')\|_1. \tag{7}$$

[2]For a ResNet18, we timed it to 15ms. Specifically, we timed the function `get_path_norm` available at `github.com/agonon/pathnorm_toolkit` using `pytorch.utils.benchmark`. The experiment was made on an NVIDIA GPU A100-40GB, with processor AMD EPYC 7742 64-Core.

Proof. For vectors a, b with $|a_i| \geqslant |b_i|$ for every i, we have

$$\|a\|_1 - \|b\|_1 = \sum_i |a_i| - |b_i| = \sum_i |a_i - b_i| = \|a - b\|_1. \qquad \square$$

An important scenario where $|\Phi(\theta)| \geqslant |\Phi(\theta')|$ indeed holds is when $|\theta| \geqslant |\theta'|$ coordinatewise. **The latter is true in at least two significant situations**: when θ' is obtained from θ by **pruning**, or through **quantization** provided that rounding is done either systematically towards zero or systematically away from zero.

Note that $|\theta| \geqslant |\theta'|$ is not the only situation where $|\Phi(\theta)| \geqslant |\Phi(\theta')|$. For instance, due to the rescaling-invariance of $\Phi(\cdot)$, if $\tilde{\theta}$ is rescaling-equivalent to θ the coordinatewise inequality $|\Phi(\tilde{\theta})| \geqslant |\Phi(\theta')|$ remains valid, even though in general such a $\tilde{\theta}$ non longer satisfies $|\tilde{\theta}| \geqslant |\theta'|$ coordinatewise.

Even out of such practical scenarios, the ℓ^1-path-metric also satisfies an *invariant* upper bound.

Lemma 3.3 (Informal version of Lemma F.3)**.** *Consider a DAG ReLU network with L layers and width W. For any parameter θ, denote by $\mathtt{N}(\theta)$ its normalized version, deduced from θ by applying rescaling-symmetries such that each neuron has its vector of incoming weights equal to 1, except for output neurons. It holds for all parameters θ, θ':*

$$\|\Phi(\theta) - \Phi(\theta')\|_1 \leqslant (W^2 + \min(\|\Phi(\theta)\|_1, \|\Phi(\theta')\|_1) \cdot LW) \|\mathtt{N}(\theta) - \mathtt{N}(\theta')\|_\infty. \tag{8}$$

The proof is in Appendix F. In all the cases of interest we consider, the lower bound (6) is exact as a consequence of Lemma 3.2. We leave it to future work to compare the lower bound with the upper bound of Lemma 3.3 in specific cases where the lower bound is inexact.

3.3 Improvement over previous Lipschitz bounds

Inequality (5) improves on the Lipschitz bound (1) specified with Equation (2), as the next result shows.

Lemma 3.4. *Consider a simple layered fully-connected neural network architecture with $L \geqslant 1$ layers, corresponding to functions $R_\theta(x) = M_L \,\mathrm{ReLU}(M_{L-1} \dots \mathrm{ReLU}(M_1 x))$ with each M_ℓ denoting a matrix, and parameters $\theta = (M_1, \dots, M_L)$. For a matrix M, denote by $\|M\|_{1,\infty}$ the maximum ℓ^1 norm of a row of M. Consider $R \geqslant 1$ and define the set Θ of parameters $\theta = (M_1, \dots, M_L)$ such that $\|M_\ell\|_{1,\infty} \leqslant R$ for every $\ell \in [\![1, L]\!]$. Then, for every parameters $\theta, \theta' \in \Theta$*

$$\|\Phi(\theta) - \Phi(\theta')\|_1 \leqslant LW^2 R^{L-1} \|\theta - \theta'\|_\infty. \tag{9}$$

Moreover the right hand-side can be arbitrarily worse that the ℓ^1-pseudo-metric in the left hand side: over all rescaling-equivalent parameters $\tilde{\theta} \sim \theta$, it holds

$$\sup_{\tilde{\theta} \sim \theta} \frac{\|\tilde{\theta} - \theta'\|_\infty}{\|\Phi(\tilde{\theta}) - \Phi(\theta')\|_1} = \infty.$$

The proof of Lemma 3.4 is in Inequality (28) in Appendix G.

The *invariant* Lipschitz bound (5) combined with (9) yields a (non-invariant) bound on $\|R_\theta(x) - R_{\theta'}(x)\|_1$:

$$\max(\|x\|_\infty, 1) LW^2 R^{L-1} \|\theta - \theta'\|_\infty.$$

In comparison the generic bound (1) specified with (2) reads

$$(W\|x\|_\infty + 1) WL^2 R^{L-1} \|\theta - \theta'\|_\infty.$$

As soon as $\|x\|_\infty \geqslant 1$ the latter is a looser bound than the former.

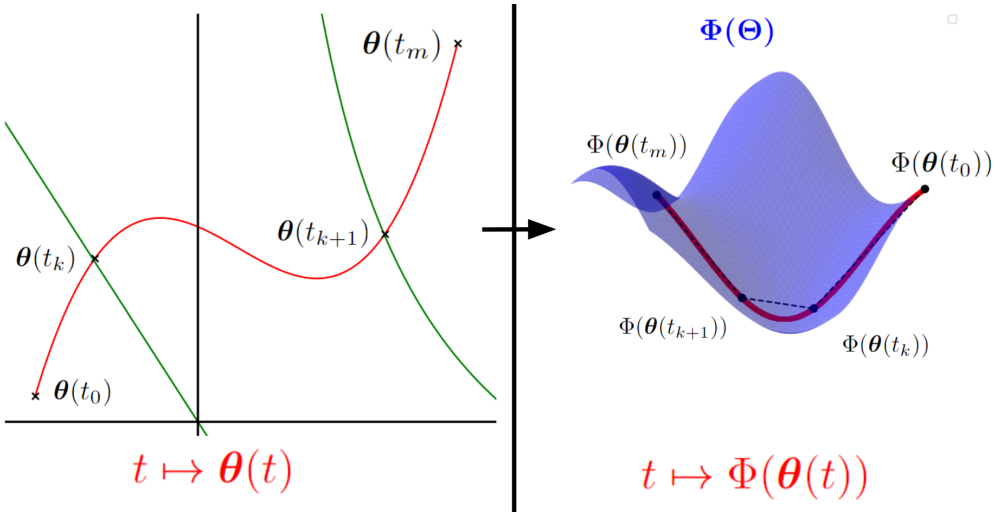

Figure 3: Illustration of the proof of Theorem 3.1, see Section 3.4 for an explanation.

3.4 Proof sketch of Theorem 3.1

Given an input x, the proof of Theorem 3.1 consists in defining a trajectory $t \in [0,1] \to \theta(t) \in \Theta$ (**red** curve in Figure 3) that starts at θ, ends at θ', and with finitely many breakpoints $0 = t_0 < t_1 < \cdots < t_m = 1$ such that the path-activations $A(\theta(t), x)$ are constant on the open intervals $t \in (t_k, t_{k+1})$. Each breakpoint corresponds to a value where the activation of at least one path (hence at least one neuron) changes in the neighborhood of $\theta(t)$. For instance, in the left part of Figure 3, the straight **green** line (resp. quadratic **green** curve) corresponds to a change of activation of a ReLU neuron (for a given input x to the network) in the first (resp. second) layer.

With such a trajectory, given the key property (4), each quantity $|R_{\theta(t_k)}(x) - R_{\theta(t_{k+1})}(x)|$ can be controlled in terms of $\|\Phi(\theta(t_k)) - \Phi(\theta(t_{k+1}))\|_1$, and if the path is "nice enough", then this control can be extended globally from t_0 to t_m.

There are two obstacles: 1) proving that there are finitely many breakpoints t_k as above (think of $t \mapsto t^{n+2}\sin(1/t)$ that is n-times continuously differentiable but still crosses $t = 0$ an infinite number of times around zero), and 2) proving that the length $\sum_{k=1}^{m} \|\Phi(\theta(t_k)) - \Phi(\theta(t_{k+1}))\|_1$ of the broken line with vertices $\Phi(\theta(t_k))$ (dashed line on the right part of Figure 3) is bounded from above by $\|\Phi(\theta) - \Phi(\theta')\|_1$ times a reasonable factor. Trajectories satisfying these two properties are called "admissible" trajectories.

The first property is true as soon as the trajectory $t \mapsto \theta(t)$ is smooth enough (analytic, say). For this, we will notably exploit that the output of a ReLU neuron in the d-th layer of a layered fully-connected network is a piecewise polynomial function of the parameters θ of degree at most d [Gonon et al., 2024, consequence of Lemma A.1], [Bona-Pellissier et al., 2022, consequence of Propositions 1 and 2]. The property second is true *with factor one* thanks to a monotonicity property of the chosen trajectory.

The core of the proof consists in exhibiting a trajectory with these two properties. To the best of our knowledge, the proof of Inequality (3) is the first to *practically leverage the idea of "adequately navigating" through the different regions in θ where the network is polynomial*[3] by respecting the geometry induced by Φ, see Figure 3 for an illustration.

4 Rescaling-invariant pruning

We use Inequality (3) to derive a new pruning algorithm that is both effective and invariant under symmetries. Instead of taking pruning decisions based on a criterion in the parameter space, e.g., based on the magnitude of the weights, we propose to prune based on the ℓ^1-path-metric. We show this to match the accuracy of

[3]The mapping $(\theta, x) \mapsto R_\theta(x)$ is indeed known to be piecewise polynomial in the coordinates of θ [Gonon et al., 2024, consequence of Lemma A.1][Bona-Pellissier et al., 2022, consequence of Propositions 1 and 2].

magnitude pruning when applied to ResNets trained on Imagenet in the lottery ticket context [Frankle et al., 2020], while being rescaling-invariant.

4.1 Pruning: a quick overview

Pruning typically involves ranking weights by a chosen criterion and removing (setting to zero) those deemed less important Han et al. [2016]. Early criteria considered either weight magnitudes Han et al. [2016], Hanson and Pratt [1988] or the loss's sensitivity to each weight Hassibi and Stork [1992], LeCun et al. [1989]. Building on these foundations, more sophisticated pruning methods have emerged, often formulated as complex optimization problems solved via advanced algorithms. For example, consider the *entrywise* loss's sensitivity criterion of [LeCun et al., 1989]. In principle, all the costs should be recomputed after each pruning decision, since removing one weight affects the costs of the others. A whole literature focuses on turning the cost of [LeCun et al., 1989] into an algorithm that would take into account these global dependencies Benbaki et al. [2023], Singh and Alistarh [2020], Yu et al. [2022]. This line of work recently culminated in CHITA Benbaki et al. [2023], a pruning approach that scales up to millions of parameters through substantial engineering effort.

Here, we introduce a *path-magnitude* cost defined for each *individual weight* but that depends on the *global* configuration of the weights. Just as sensitivity-based costs LeCun et al. [1989], these costs should in principle be re-computed after each pruning decision. While taking these global dependencies into account is expected to provide better performance, this is also expected to require a huge engineering effort, similar to what has been done in Benbaki et al. [2023], Singh and Alistarh [2020], Yu et al. [2022], which is beyond the scope of this paper. Our goal here is more modest: we aim at providing a simple proof-of-concept to show the promises of the path-lifting for *rescaling-invariant* pruning.

Table 2: Comparison of pruning criteria across key properties. Being *data-specific* or *loss-specific* can be both a strength (leveraging the training loss and data for more accurate pruning) and a limitation (requiring access to additional information). Being *rescaling-invariant* ensures the pruning mask is unaffected by neuron-wise weight rescaling.

Criterion	Rescaling-Invariant	Error bound	Data-Specific	Loss-Specific	Efficient to Compute	Versatile[a]
Magnitude	No	Yes – (1)-(2)	No	No	Yes	Yes
Loss-Sensitivity (Taylor Expansion)	Yes in theory Not in practice[c]	No	Yes	Yes	Depends[b]	Yes
Path-Magnitude	Yes	Yes – (13)	No	No	Yes	Yes

[a] Can be used to design greedy approaches (including ℓ^0-based methods) and supports both structured and unstructured pruning.
[b] Depends on how higher-order derivatives of the loss are taken into account. E.g., using only the diagonal of the Hessian can be relatively quick, but computing the full Hessian is infeasible for large networks. See Table 3 for experiments.
[c] See Equation (21) in Appendix E for invariance in theory, and end of Appendix E for non-invariance in practice.

Notion of pruned parameter. Considering a neural network architecture given by a graph G, we use the shorthand $\mathbb{R}^G$ to denote the corresponding set of parameters (see Definition A.2 for a precise definition). By definition, a pruned version θ' of $\theta \in \mathbb{R}^G$ is a "Hadamard" product $\theta' = s \odot \theta$, where $s \in \{0,1\}^G$ and $\|s\|_0$ is "small". We denote $\mathbf{1}_G \in \mathbb{R}^G$ the vector filled with ones, $e_i \in \mathbb{R}^G$ the i-th canonical vector, $s_i := \mathbf{1}_G - e_i$, and introduce the specialized notation $\theta_{-i} := s_i \odot \theta$ for the vector where a single entry (the weight of an edge or the bias of a hidden or output neuron) of θ, indexed by i, is set to zero.

4.2 Proposed rescaling-invariant pruning criterion

The starting point of the proposed pruning criterion is that, given any θ, the pair θ, θ' with $\theta' := s \odot \theta$ satisfies the assumptions of Theorem 3.1, hence for all input x we have $|R_\theta(x) - R_{\theta'}(x)| \leqslant \|\Phi(\theta) - \Phi(\theta')\|_1 \max(1, \|x\|_\infty)$. Specializing this observation to the case where a single entry (the weight of an edge, or the bias of hidden or

output neuron indexed by i) of θ is pruned (*i.e.*, $\theta' = \theta_{-i}$) suggests the following definition, which will serve as a *pruning criterion*:

Definition 4.1. We denote

$$\texttt{Path-Mag}(\theta, i) := \|\Phi(\theta) - \Phi(\theta_{-i})\|_1. \tag{10}$$

This measures the contribution to the path-norm of all paths p containing entry i: when $i \notin p$ we have $\Phi_p(\theta_{-i}) = \Phi_p(\theta)$, while otherwise $\Phi_p(\theta_{-i}) = 0$. Since θ and θ_{-i} satisfy the assumptions of Lemma 3.2 we have

$$\begin{aligned}\texttt{Path-Mag}(\theta, i) &\underset{(7)}{=} \|\Phi(\theta)\|_1 - \|\Phi(\theta_{-i})\|_1 \qquad (11)\\ &= \sum_{p\in\mathcal{P}} |\Phi_p(\theta)| - \sum_{p\in\mathcal{P}: i\notin p} |\Phi_p(\theta)| \\ &= \sum_{p\in\mathcal{P}: i\in p} |\Phi_p(\theta)| \qquad (12)\end{aligned}$$

In light of (5), to limit the impact of pruning on the perturbation of the initial function R_θ, it is natural to choose a coordinate i of θ leading to a small value of this criterion.

Lemma 4.2. `Path-Mag` *enjoys the following properties:*

- **rescaling-invariance***: for each $\theta \in \mathbb{R}^G$ and index i,* $\texttt{Path-Mag}(\theta, i) = \texttt{Path-Mag}(\tilde{\theta}, i)$ *for every rescaling-equivalent parameters $\tilde{\theta} \sim \theta$;*
- **error bound:** *denote $s := \mathbf{1}_G - \sum_{i\in I} e_i$ where I indexes entries of $\theta \in \mathbb{R}^G$ to be pruned. We have*

$$\begin{aligned}&|R_\theta(x) - R_{s\odot\theta}(x)| \\ &\quad\leqslant \Big(\sum_{i\in I} \texttt{Path-Mag}(\theta, i)\Big) \max(1, \|x\|_\infty).\end{aligned} \tag{13}$$

- **computation with only two forward passes***: using Equation (11) and the fact that $\|\Phi(\cdot)\|_1$ is computable in one forward pass Gonon et al. [2024].*
- **efficient joint computation *for all entries*:** *we have*

$$(\texttt{Path-Mag}(\theta, i))_i = \theta \odot \nabla_\theta \|\Phi(\theta)\|_1 \tag{14}$$

that enables computation via auto-differentiation.

The proof is given in Appendix C. We summarize these properties in Table 2.

4.3 Considered (basic) path-magnitude pruning method

Equipped with `Path-Mag`, a basic rescaling-invariant pruning approach is to minimize the upper-bound (13). This is achieved via simple *reverse* hard thresholding:

1. compute $\texttt{Path-Mag}(\theta, i)$ for all i (two forward passes per i via Equation (11); more efficiently a single pass of autodifferentiation via Equation (14));
2. prune out the entries of θ corresponding to the indices yielding the *smallest values* of this cost.

To the best of our knowledge, this is the first practical network pruning method that is both *invariant* under rescaling symmetries and *endowed with guarantees* such as (11) on modern networks.

While Table 3 shows that path-magnitude pruning is *computationally feasible*, we must also verify that when injected in usual pruning pipelines, it yields *acceptable accuracies*.

As a simple proof-of-concept, we train a dense ResNet-18 on ImageNet-1k with standard hyperparameters, prune with the proposed path-magnitude pruning method a prescribed percentage p of the weights, rewind the weights to their value after a few epochs (as in the lottery ticket literature [Frankle et al., 2020]) and

Table 3: Times (in milliseconds) to compute the pruning cost of all weights at once for standard networks. We include the time of a forward pass for reference. The entries in the "Loss-sensitivity via Optimal Brain Damage (OBD)" and "Forward" columns show times for batch sizes of 1 and 128 (e.g., "13–60" means 13 ms at batch size 1 vs. 60 ms at batch size 128). See Appendix E for details.

Network	**Forward**	**Magnitude**	**Loss-sensitivity via OBD [LeCun et al., 1989]**	**Path-Magnitude**
AlexNet (61M)	1.7-133	0.5	13-60	14
VGG16 (138M)	2.3-198	1.4	31-675	61
ResNet18 (12M)	3.6-142	3.2	51-155	32

then retrain the pruned network from these weights' value. We do the same with magnitude pruning. We find both pruning methods to yield the same[4] test accuracy at the end of the process when run with the same value of p between 10% and 80%. However, path-magnitude pruning has the advantage of being robust against arbitrary (and in particular adversary) weights rescaling that could have been applied to the original pre-trained network. Indeed, it will select the same mask. On the contrary, we experimentally observe magnitude pruning to select a different mask when random rescales are applied after the original training phase, ending up in large drops of test accuracy. See Appendix D for details.

Table 3 shows the time needed to compute this pruning criterion on some widespread ReLU networks, see Appendix E for details.

4.4 Discussion and possible future extension

The cost $\texttt{Path-Mag}(\theta, i)$ is defined per weight, but its value for a given weight indexed by i also depends on the other weights. Therefore, one could hope to achieve better pruning properties if, once a weight is pruned, the path-magnitude costs of the remaining weights were updated. This is reminiscent of the loss-sensitivity cost LeCun et al. [1989] that associates to each weight i (a surrogate of) the difference $\ell(\theta_{-i}) - \ell(\theta)$, where ℓ is a given loss function. The challenge is similar in both cases: how to account for *global* dependencies between the pruning costs associated to each *individual* weight? In this direction, a whole literature has developed techniques attempting to *globally* minimize (a surrogate of) $\ell(s \odot \theta) - \ell(\theta)$ over the (combinatorial) choice of a support s satisfying an ℓ^0-constraint. Such approaches have been scaled up to million of parameters in Benbaki et al. [2023] by combining a handful of clever algorithmic designs. Similar iterative or greedy strategies could be explored to aim at solving the (seemingly) combinatorial ℓ^0-optimization problem $\|\Phi(s \odot \theta) - \Phi(\theta)\|_1$.

5 Conclusion

We introduced a new Lipschitz bound on the distance between two neural network realizations, leveraging the path-lifting framework of Gonon et al. [2024]. By formulating this distance in terms of the ℓ^1-path-metric, our result applies to a broad class of modern ReLU networks—including ones like ResNets or AlphaGo—and crucially overcomes the arbitrary pessimism arising in non-invariant parameter-based bounds. Beyond providing a theoretical guarantee, we also argued that this metric can be computed efficiently in practical scenarios such as pruning and quantization.

We then demonstrated how to apply path-lifting to pruning: the *path-magnitude* criterion defines a rescaling-invariant measure of the overall contribution of a weight. In a proof-of-concept on a ResNet-18 trained on ImageNet, *path-magnitude* pruning yields an accuracy on par with standard magnitude pruning. This connects the theoretical notion of path-lifting to a practical goal: making pruning decisions that cannot be undermined by mere neuron-wise rescaling.

This work raises several directions for future research. First, a natural challenge is to establish sharper versions of our core result (Theorem 3.1), typically with metrics still based on the path-lifting but using ℓ^p-norms with $p > 1$, or by deriving functional bounds in expectation (over a given probability distribution of inputs).

[4]Note that these results were achieved without tuning effort: we used for both pruning methods the standard hyperparameters used for *magnitude pruning* in such situation [Frankle et al., 2021].

Second, more advanced iterative algorithms, akin to second-order pruning techniques, might benefit from path-lifting as a fundamental building block, improving upon the simple one-pass approach used in our proof-of-concept while retaining invariance properties (see Section 4.4).

Finally, although our main theorem improves existing Lipschitz bounds and extends them to a wide range of network architectures, the potential applications of the path-lifting perspective–and its invariance under rescaling–are far from exhausted. Quantization and generalization, in particular, are two important areas where the present findings might stimulate further developments on metrics that offer both theoretical grounding and compelling practical properties.

Acknowledgements

This work was supported in part by the AllegroAssai ANR-19-CHIA-0009, by the NuSCAP ANR-20-CE48-0014 projects of the French Agence Nationale de la Recherche and by the SHARP ANR project ANR-23-PEIA-0008 in the context of the France 2030 program.

The authors thank the Blaise Pascal Center for the computational means. It uses the SIDUS solution [Quemener and Corvellec, 2013] developed by Emmanuel Quemener.

References

Francis Bach. *Learning Theory from First Principles*. The MIT Press, 2024. ISBN 9780262049443. URL https://mitpress.mit.edu/9780262049443/learning-theory-from-first-principles/.

Andrew R. Barron and Jason M. Klusowski. Complexity, statistical risk, and metric entropy of deep nets using total path variation. *CoRR*, abs/1902.00800, 2019. URL http://arxiv.org/abs/1902.00800.

C. Bekas, E. Kokiopoulou, and Y. Saad. An estimator for the diagonal of a matrix. *Applied Numerical Mathematics*, 57(11):1214–1229, 2007. ISSN 0168-9274. doi: https://doi.org/10.1016/j.apnum.2007.01.003. URL https://www.sciencedirect.com/science/article/pii/S0168927407000244. Numerical Algorithms, Parallelism and Applications (2).

Riade Benbaki, Wenyu Chen, Xiang Meng, Hussein Hazimeh, Natalia Ponomareva, Zhe Zhao, and Rahul Mazumder. Fast as CHITA: neural network pruning with combinatorial optimization. In Andreas Krause, Emma Brunskill, Kyunghyun Cho, Barbara Engelhardt, Sivan Sabato, and Jonathan Scarlett, editors, *International Conference on Machine Learning, ICML 2023, 23-29 July 2023, Honolulu, Hawaii, USA*, volume 202 of *Proceedings of Machine Learning Research*, pages 2031–2049. PMLR, 2023. URL https://proceedings.mlr.press/v202/benbaki23a.html.

Julius Berner, Philipp Grohs, and Arnulf Jentzen. Analysis of the generalization error: Empirical risk minimization over deep artificial neural networks overcomes the curse of dimensionality in the numerical approximation of black-scholes partial differential equations. *SIAM J. Math. Data Sci.*, 2(3):631–657, 2020. doi: 10.1137/19M125649X. URL https://doi.org/10.1137/19M125649X.

Joachim Bona-Pellissier, François Malgouyres, and François Bachoc. Local identifiability of deep relu neural networks: the theory. In Sanmi Koyejo, S. Mohamed, A. Agarwal, Danielle Belgrave, K. Cho, and A. Oh, editors, *Advances in Neural Information Processing Systems 35: Annual Conference on Neural Information Processing Systems 2022, NeurIPS 2022, New Orleans, LA, USA, November 28 - December 9, 2022*, 2022. URL http://papers.nips.cc/paper_files/paper/2022/hash/b0ae046e198a5e43141519868a959c74-Abstract-Conference.html.

Thomas H. Cormen, Charles E. Leiserson, Ronald L. Rivest, and Clifford Stein. *Introduction to Algorithms, 3rd Edition*. MIT Press, 2009. ISBN 978-0-262-03384-8. URL http://mitpress.mit.edu/books/introduction-algorithms.

Ronald A. DeVore, Boris Hanin, and Guergana Petrova. Neural network approximation. *Acta Numer.*, 30:327–444, 2021. doi: 10.1017/S0962492921000052. URL https://doi.org/10.1017/S0962492921000052.

Jonathan Frankle, David J. Schwab, and Ari S. Morcos. The early phase of neural network training. In *8th International Conference on Learning Representations, ICLR 2020, Addis Ababa, Ethiopia, April 26-30, 2020*. OpenReview.net, 2020. URL https://openreview.net/forum?id=Hkl1iRNFwS.

Jonathan Frankle, Gintare Karolina Dziugaite, Daniel M. Roy, and Michael Carbin. Pruning neural networks at initialization: Why are we missing the mark? In *9th International Conference on Learning Representations, ICLR 2021, Virtual Event, Austria, May 3-7, 2021*. OpenReview.net, 2021. URL https://openreview.net/forum?id=Ig-VyQc-MLK.

Antoine Gonon. *Harnessing symmetries for modern deep learning challenges : a path-lifting perspective*. Theses, Ecole normale supérieure de lyon - ENS LYON, November 2024. URL https://theses.hal.science/tel-04784426.

Antoine Gonon, Nicolas Brisebarre, Rémi Gribonval, and Elisa Riccietti. Approximation speed of quantized versus unquantized relu neural networks and beyond. *IEEE Trans. Inf. Theory*, 69(6):3960–3977, 2023. doi: 10.1109/TIT.2023.3240360. URL https://doi.org/10.1109/TIT.2023.3240360.

Antoine Gonon, Nicolas Brisebarre, Elisa Riccietti, and Rémi Gribonval. A path-norm toolkit for modern networks: consequences, promises and challenges. In *International Conference on Learning Representations, ICLR 2024 Spotlight, Vienna, Austria, May 7-11*. OpenReview.net, 2024. URL https://openreview.net/pdf?id=hiHZVUIYik.

Song Han, Huizi Mao, and William J. Dally. Deep compression: Compressing deep neural network with pruning, trained quantization and huffman coding. In Yoshua Bengio and Yann LeCun, editors, *4th International Conference on Learning Representations, ICLR 2016, San Juan, Puerto Rico, May 2-4, 2016, Conference Track Proceedings*, 2016. URL http://arxiv.org/abs/1510.00149.

Stephen Jose Hanson and Lorien Y. Pratt. Comparing biases for minimal network construction with back-propagation. In David S. Touretzky, editor, *Advances in Neural Information Processing Systems 1, [NIPS Conference, Denver, Colorado, USA, 1988]*, pages 177–185. Morgan Kaufmann, 1988. URL http://papers.nips.cc/paper/156-comparing-biases-for-minimal-network-construction-with-back-propagation.

Babak Hassibi and David G. Stork. Second order derivatives for network pruning: Optimal brain surgeon. In Stephen Jose Hanson, Jack D. Cowan, and C. Lee Giles, editors, *Advances in Neural Information Processing Systems 5, [NIPS Conference, Denver, Colorado, USA, November 30 - December 3, 1992]*, pages 164–171. Morgan Kaufmann, 1992. URL http://papers.nips.cc/paper/647-second-order-derivatives-for-network-pruning-optimal-brain-surgeon.

Kaiming He, Xiangyu Zhang, Shaoqing Ren, and Jian Sun. Deep residual learning for image recognition. In *2016 IEEE Conference on Computer Vision and Pattern Recognition, CVPR 2016, Las Vegas, NV, USA, June 27-30, 2016*, pages 770–778. IEEE Computer Society, 2016. doi: 10.1109/CVPR.2016.90. URL https://doi.org/10.1109/CVPR.2016.90.

Kenji Kawaguchi, Leslie Pack Kaelbling, and Yoshua Bengio. Generalization in deep learning. *CoRR*, abs/1710.05468, 2017. URL http://arxiv.org/abs/1710.05468.

Yann LeCun, John S. Denker, and Sara A. Solla. Optimal brain damage. In David S. Touretzky, editor, *Advances in Neural Information Processing Systems 2, [NIPS Conference, Denver, Colorado, USA, November 27-30, 1989]*, pages 598–605. Morgan Kaufmann, 1989. URL http://papers.nips.cc/paper/250-optimal-brain-damage.

Sibylle Marcotte, Rémi Gribonval, and Gabriel Peyré. Abide by the law and follow the flow: Conservation laws for gradient flows. *CoRR*, abs/2307.00144, 2023. doi: 10.48550/arXiv.2307.00144. URL https://doi.org/10.48550/arXiv.2307.00144.

Behnam Neyshabur, Ryota Tomioka, and Nathan Srebro. Norm-based capacity control in neural networks. In Peter Grünwald, Elad Hazan, and Satyen Kale, editors, *Proceedings of The 28th Conference on Learning*

Theory, COLT 2015, Paris, France, July 3-6, 2015, volume 40 of *JMLR Workshop and Conference Proceedings*, pages 1376–1401. JMLR.org, 2015. URL http://proceedings.mlr.press/v40/Neyshabur15.html.

Behnam Neyshabur, Srinadh Bhojanapalli, and Nathan Srebro. A PAC-Bayesian approach to spectrally-normalized margin bounds for neural networks. In *6th International Conference on Learning Representations, ICLR 2018, Vancouver, BC, Canada, April 30 - May 3, 2018, Conference Track Proceedings*. OpenReview.net, 2018. URL https://openreview.net/forum?id=Skz_WfbCZ.

E. Quemener and M. Corvellec. Sidus—the solution for extreme deduplication of an operating system. *Linux Journal*, 2013.

Shai Shalev-Shwartz and Shai Ben-David. *Understanding Machine Learning - From Theory to Algorithms*. Cambridge University Press, 2014. ISBN 978-1-10-705713-5. URL http://www.cambridge.org/de/academic/subjects/computer-science/pattern-recognition-and-machine-learning/understanding-machine-learning-theory-algorithms.

Sidak Pal Singh and Dan Alistarh. Woodfisher: Efficient second-order approximation for neural network compression. In Hugo Larochelle, Marc'Aurelio Ranzato, Raia Hadsell, Maria-Florina Balcan, and Hsuan-Tien Lin, editors, *Advances in Neural Information Processing Systems 33: Annual Conference on Neural Information Processing Systems 2020, NeurIPS 2020, December 6-12, 2020, virtual*, 2020. URL https://proceedings.neurips.cc/paper/2020/hash/d1ff1ec86b62cd5f3903ff19c3a326b2-Abstract.html.

Pierre Stock and Rémi Gribonval. An embedding of ReLU networks and an analysis of their identifiability. *Constr. Approx.*, 57(2):853–899, 2023. ISSN 0176-4276,1432-0940. doi: 10.1007/s00365-022-09578-1. URL https://doi.org/10.1007/s00365-022-09578-1.

Xin Yu, Thiago Serra, Srikumar Ramalingam, and Shandian Zhe. The combinatorial brain surgeon: Pruning weights that cancel one another in neural networks. In Kamalika Chaudhuri, Stefanie Jegelka, Le Song, Csaba Szepesvári, Gang Niu, and Sivan Sabato, editors, *International Conference on Machine Learning, ICML 2022, 17-23 July 2022, Baltimore, Maryland, USA*, volume 162 of *Proceedings of Machine Learning Research*, pages 25668–25683. PMLR, 2022. URL https://proceedings.mlr.press/v162/yu22f.html.

Appendices

A Path-lifting and path-activations

This section recalls the definitions from Gonon et al. [2024] for completeness.

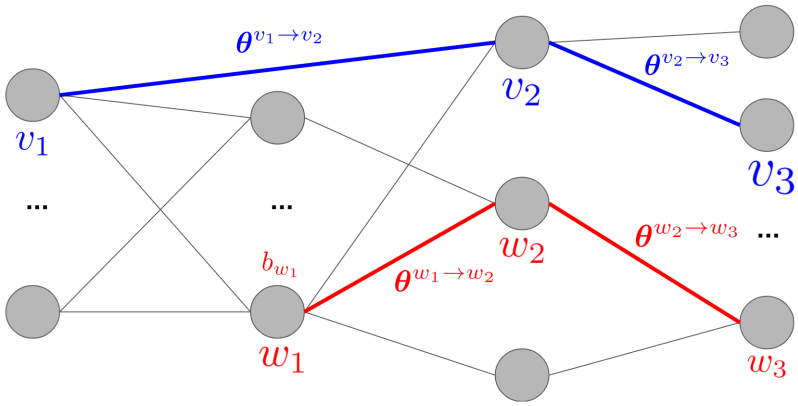

$$\boldsymbol{A}(\theta, x) = \begin{array}{c} \\ \mathcal{P}_I \left\{ \begin{array}{c} p \end{array} \right. \\ \\ \mathcal{P}_H \left\{ \begin{array}{c} p' \end{array} \right. \end{array} \begin{array}{c} \overbrace{\qquad\qquad\qquad\qquad}^{N_{\text{in}}} \quad b \\ v_1 \\ \cdots \\ \left(\begin{array}{ccccccc|c} 0 & \ldots & 0 & a_p(\theta, x) & 0 & \ldots & 0 & 0 \\ \cdots & & & & & & & \\ \hline & & & & & & & \vdots \\ & & & 0 & & & & a_{p'}(\theta, x) \\ & & & & & & & \vdots \end{array} \right) \end{array}$$

Figure 4: The coordinate of the path-lifting Φ associated with the path $p = v_1 \to v_2 \to v_3$ is $\Phi_p(\theta) = \theta^{v_1 \to v_2} \theta^{v_2 \to v_3}$ since it starts from an input neuron (Definition A.5). While the path $p' = w_1 \to w_2 \to w_3$ starts from a hidden neuron (in $N \setminus (N_{\text{in}} \cup N_{\text{out}})$), so there is also the bias of w_1 to take into account: $\Phi_{p'}(\theta) = b_{w_1} \theta^{w_1 \to w_2} \theta^{w_2 \to w_3}$. As specified in Definition A.5, the columns of the path-activation matrix $\boldsymbol{A}$ are indexed by $N_{\text{in}} \cup \{b\}$ and its rows are indexed by $\mathcal{P} = \mathcal{P}_I \cup \mathcal{P}_H$, with $\mathcal{P}_I$ the set of paths in $\mathcal{P}$ starting from an input neuron, and $\mathcal{P}_H$ the set of paths starting from a hidden neuron.

Definition A.1 (ReLU and k-max-pooling activation functions)**.** The ReLU function is defined as $\text{ReLU}(x) := x\mathbb{1}_{x \geqslant 0}$ for $x \in \mathbb{R}$. The k-max-pooling function $k\text{-}\texttt{pool}(x) := x_{(k)}$ returns the k-th largest coordinate of $x \in \mathbb{R}^d$.

Definition A.2 (ReLU neural network [Gonon et al., 2024])**.** Consider a Directed Acyclic Graph (DAG) $G = (N, E)$ with edges E, and vertices N called neurons. For a neuron v, the sets $\text{ant}(v), \text{suc}(v)$ of antecedents and successors of v are $ant(v) := \{u \in N, u \to v \in E\}, \text{suc}(v) := \{u \in N, v \to u \in E\}$. Neurons with no antecedents (resp. no successors) are called input (resp. output) neurons, and their set is denoted N_{in} (resp. N_{out}). Neurons in $N \setminus (N_{\text{in}} \cup N_{\text{out}})$ are called hidden neurons. Input and output dimensions are respectively $d_{\text{in}} := |N_{\text{in}}|$ and $d_{\text{out}} := |N_{\text{out}}|$.

• A **ReLU neural network architecture** is a tuple $(G, (\rho_v)_{v \in N \setminus N_{\text{in}}})$ composed of a DAG $G = (N, E)$ with attributes $\rho_v \in \{\text{id}, \text{ReLU}\} \cup \{k\text{-}\texttt{pool}, k \in \mathbb{N}_{>0}\}$ for $v \in N \setminus (N_{\text{out}} \cup N_{\text{in}})$ and $\rho_v = \text{id}$ for $v \in N_{\text{out}}$.

We will again denote the tuple $(G, (\rho_v)_{v \in N \setminus N_{\text{in}}})$ by G, and it will be clear from context whether the results depend only on $G = (N, E)$ or also on its attributes. Define $N_\rho := \{v \in N, \rho_v = \rho\}$ for an activation ρ, and $N_{*\texttt{-pool}} := \cup_{k \in \mathbb{N}_{>0}} N_{k\texttt{-pool}}$. A neuron in $N_{*\texttt{-pool}}$ is called a $*$-max-pooling neuron. For $v \in N_{*\texttt{-pool}}$, its kernel size is defined as being $|\operatorname{ant}(v)|$.

• **Parameters** associated with this architecture are vectors[5] $\theta \in \mathbb{R}^G := \mathbb{R}^{E \cup N \setminus N_{\text{in}}}$. We call bias $b_v := \theta_v$ the coordinate associated with a neuron v (input neurons have no bias), and denote $\theta^{u \to v}$ the weight associated with an edge $u \to v \in E$. We will often denote $\theta^{\to v} := (\theta^{u \to v})_{u \in \operatorname{ant}(v)}$ and $\theta^{v \to} := (\theta^{u \to v})_{u \in \operatorname{suc}(v)}$.

• The **realization** of a neural network with parameters $\theta \in \mathbb{R}^G$ is the function $R_\theta^G : \mathbb{R}^{N_{\text{in}}} \to \mathbb{R}^{N_{\text{out}}}$ (simply denoted R_θ when G is clear from the context) defined for every input $x \in \mathbb{R}^{N_{\text{in}}}$ as

$$R_\theta(x) := (v(\theta, x))_{v \in N_{\text{out}}},$$

where we use the same symbol v to denote a neuron $v \in N$ and the associated function $v(\theta, x)$, defined as $v(\theta, x) := x_v$ for an input neuron v, and defined by induction otherwise

$$v(\theta, x) := \begin{cases} \rho_v(b_v + \sum_{u \in \operatorname{ant}(v)} u(\theta, x)\theta^{u \to v}) & \text{if } \rho_v = \text{ReLU or } \rho_v = \text{id}, \\ k\texttt{-pool}\left((b_v + u(\theta, x)\theta^{u \to v})_{u \in \operatorname{ant}(v)}\right) & \text{if } \rho_v = k\texttt{-pool}. \end{cases}$$

Definition A.3 (Paths and depth in a DAG [Gonon et al., 2024])**.** Consider a DAG $G = (N, E)$ as in Definition A.2. A path of G is any sequence of neurons $v_0, \ldots, v_d$ such that each $v_i \to v_{i+1}$ is an edge in G. Such a path is denoted $p = v_0 \to \ldots \to v_d$. This includes paths reduced to a single $v \in N$, denoted $p = v$. The *length* of a path is $\texttt{length}(p) = d$ (the number of edges). We will denote $p_\ell := v_\ell$ the ℓ-th neuron for a general $\ell \in \{0, \ldots, \texttt{length}(p)\}$ and use the shorthand $p_{\texttt{end}} = v_{\texttt{length}(p)}$ for the last neuron. The *depth of the graph* G is the maximum length over all of its paths. If $v_{d+1} \in \operatorname{suc}(p_{\texttt{end}})$ then $p \to v_{d+1}$ denotes the path $v_0 \to \ldots \to v_d \to v_{d+1}$. We denote by $\mathcal{P}^G$ (or simply $\mathcal{P}$) the set of paths ending at an output neuron of G.

Definition A.4 (Sub-graph ending at a given neuron)**.** Given a neuron v of a DAG G, we denote $G^{\to v}$ the graph deduced from G by keeping only the largest subgraph with the same inputs as G and with v as a single output: every neuron u with no path to reach v through the edges of G is removed, as well as all its incoming and outcoming edges. We will use the shorthand $\mathcal{P}^{\to v} := \mathcal{P}^{G^{\to v}}$ to denote the set of paths in G ending at v.

We now recall the definitions of the path-lifting and path-activations from Gonon et al. [2024]. An illustration can be found in Figure 4.

Definition A.5 (Path-lifting and path-activations [Gonon et al., 2024])**.** Consider a ReLU neural network architecture G as in Definition A.2 and parameters $\theta \in \mathbb{R}^G$ associated with G. For $p \in \mathcal{P}$, define

$$\Phi_p(\theta) := \begin{cases} \prod_{\ell=1}^{\texttt{length}(p)} \theta^{v_{\ell-1} \to v_\ell} & \text{if } p_0 \in N_{\text{in}}, \\ b_{p_0} \prod_{\ell=1}^{\texttt{length}(p)} \theta^{v_{\ell-1} \to v_\ell} & \text{otherwise,} \end{cases}$$

where an empty product is equal to 1 by convention. The path-lifting $\Phi^G(\theta)$ of θ is

$$\Phi^G(\theta) := (\Phi_p(\theta))_{p \in \mathcal{P}^G}.$$

This is often denoted Φ when the graph G is clear from the context. We will use the shorthand $\Phi^{\to v} := \Phi^{G^{\to v}}$ to denote the path-lifting associated with $G^{\to v}$ (Definition A.4).

Consider an input x of G. The activation of an *edge* $u \to v$ on (θ, x) is defined to be $a_{u \to v}(\theta, x) := 1$ when v is an identity neuron; $a_{u \to v}(\theta, x) := \mathbb{1}_{v(\theta,x)>0}$ when v is a ReLU neuron; and when v is a k-max-pooling neuron, define $a_{u \to v}(\theta, x) := 1$ if the neuron u is the first in $\operatorname{ant}(v)$ in lexicographic order to satisfy $u(\theta, x) := k\texttt{-pool}\left((w(\theta, x))_{w \in \operatorname{ant}(v)}\right)$ and $a_{u \to v}(\theta, x) := 0$ otherwise. The activation of a *neuron* v on (θ, x) is defined to be $a_v(\theta, x) := 1$ if v is an input neuron, an identity neuron, or a k-max-pooling neuron, and $a_v(\theta, x) := \mathbb{1}_{v(\theta,x)>0}$ if v is a ReLU neuron. We then define the activation of a *path* $p \in \mathcal{P}$ with respect to input

[5] For an index set I, denote $\mathbb{R}^I = \{(\theta_i)_{i \in I}, \theta_i \in \mathbb{R}\}$.

x and parameters θ as: $a_p(\theta,x) := a_{p_0}(\theta,x)\prod_{\ell=1}^{\mathtt{length}(p)} a_{v_{\ell-1}\to v_\ell}(\theta,x)$ (with an empty product set to one by convention). Consider a new symbol $v_{\mathtt{bias}}$ that is not used for denoting neurons. The path-activations matrix $\boldsymbol{A}(\theta,x)$ is defined as the matrix in $\mathbb{R}^{\mathcal{P}\times(N_{\mathrm{in}}\cup\{v_{\mathtt{bias}}\})}$ such that for any path $p\in\mathcal{P}$ and neuron $u\in N_{\mathrm{in}}\cup\{v_{\mathtt{bias}}\}$

$$(\boldsymbol{A}(\theta,x))_{p,u} := \begin{cases} a_p(\theta,x)\mathbb{1}_{p_0=u} & \text{if } u\in N_{\mathrm{in}},\\ a_p(\theta,x)\mathbb{1}_{p_0\notin N_{\mathrm{in}}} & \text{otherwise when } u=v_{\mathtt{bias}}.\end{cases}$$

B Proof of Theorem 3.1

We actually prove the next theorem that is stronger than Theorem 3.1. We do not state it in the main body as it requires having in mind the definition of the path-lifting Φ, recalled in Definition A.5, to understand the following notations. For parameters θ, we will denote $\Phi^I(\theta)$ (resp. $\Phi^H(\theta)$) the sub-vector of $\Phi(\theta)$ corresponding to the coordinates associated with paths starting from an input (resp. hidden) neuron. Thus, $\Phi(\theta)$ is the concatenation of $\Phi^I(\theta)$ and $\Phi^H(\theta)$.

Theorem B.1. *Consider a ReLU neural network as in Definition A.2, with output dimension equal to one. Consider associated parameters θ,θ'. If for every coordinate i, θ_i and θ'_i have the same signs or at least one of them is zero ($\theta_i\theta'_i\geqslant 0$), we have for every input x:*

$$|R_\theta(x)-R_{\theta'}(x)| \leqslant \|x\|_\infty \|\Phi^I(\theta)-\Phi^I(\theta')\|_1 + \|\Phi^H(\theta)-\Phi^H(\theta')\|_1. \tag{15}$$

Moreover, for every neural network architecture, there are parameters $\theta\neq\theta'$ and an input x such that Inequality (5) is an equality.

Theorem B.1 is intentionally stated with scalar output in order to let the reader deduce the result with multi-dimensional output with his favorite norm. As an example, we derive the next corollary, which corresponds to the Theorem 3.1 given in the text body (except for the equality case, which is also an easy consequence of the equality case of Inequality (15)).

Corollary B.2. *Consider an exponent $q\in[1,\infty)$ and a ReLU neural network as in Definition A.2. Consider associated parameters θ,θ'. If for every coordinate i, it holds $\theta_i\theta'_i\geqslant 0$, then for every input $x\in\mathbb{R}^{d_{in}}$:*

$$\|R_\theta(x)-R_{\theta'}(x)\|_q \leqslant \max(\|x\|_\infty,1)\|\Phi(\theta)-\Phi(\theta')\|_1.$$

Proof of Corollary B.2. By definition of the model, it holds:

$$\|R_\theta(x)-R_{\theta'}(x)\|_q^q = \sum_{v\in N_{\mathrm{out}}} |v(\theta,x)-v(\theta',x)|^q.$$

Recall that $\Phi^{\to v}$ is the path-lifting associated with the sub-graph $G^{\to v}$ (Definition A.5). By Theorem B.1, it holds:

$$|v(\theta,x)-v(\theta',x)|^q \leqslant \max(\|x\|_\infty^q,1)\|\Phi^{\to v}(\theta)-\Phi^{\to v}(\theta')\|_1^q.$$

Since $\Phi(\theta)=(\Phi^{\to v}(\theta))_{v\in N_{\mathrm{out}}}$, this implies:

$$\|R_\theta(x)-R_{\theta'}(x)\|_q^q \leqslant \max(\|x\|_\infty^q,1)\|\Phi(\theta)-\Phi(\theta')\|_1^q. \qquad \square$$

Figure 5: Counter-example showing that the conclusion of Theorem 3.1 does not hold when the parameters have opposite signs. If the hidden neurons are ReLU neurons, the left network implements $R_\theta(x)=\mathrm{ReLU}(x)$ (with $\theta=(1\quad 1)^T$) and the right network implements $R_{\theta'}(x)=-\mathrm{ReLU}(-x)$ (with $\theta'=(-1\quad -1)^T$). Inequality (5) does not hold since there is a single path and the product of the weights along this path is equal to one in both cases, so that $\Phi(\theta)=\Phi(\theta')=1$ (cf Section 2) while these two functions are nonzero and have disjoint supports.

Sketch of the proof of Theorem B.1. To prove the inequality, we define the notion of admissible trajectory, show that it is enough to find an admissible trajectory in order to conclude (Lemma B.3), and then we construct such an admissible trajectory (Corollary B.6). A geometric illustration of the spirit of the proof is given in Figure 3, as detailed in the figure legend. The formal proof of Theorem B.1, including the equality case, is given at the end of the section.

Admissible trajectory: definition. Given any input vector x and two parameters θ, θ', we define an *x-admissible trajectory*[6] betweeen θ and θ' as any continuous map $t \in [0,1] \mapsto \theta(t)$ such that for every $t \in [0,1]$, the vector $\theta(t)$ corresponds to parameters associated with the considered network architecture, with the boundary conditions $\theta(0) = \theta$ and $\theta(1) = \theta'$, and with the additional "x-admissibility property" corresponding to the existence of *finitely many* breakpoints $0 = t_0 < t_1 < \cdots < t_m = 1$ such that the path-activations matrix (see Definition A.5) $t \in [0,1] \mapsto \boldsymbol{A}(\theta(t), x)$ is constant on each interval (t_k, t_{k+1}) and such that for every path p of the graph, using the shorthand $\theta_k := \theta(t_k)$, the "reverse triangle inequality" holds (which is then, of course, an equality):

$$\sum_{k=1}^{m} |\Phi_p(\theta_k) - \Phi_p(\theta_{k-1})| \leqslant |\Phi_p(\theta_m) - \Phi_p(\theta_0)|. \tag{16}$$

Finding an admissible trajectory is enough.

Lemma B.3. *Consider an input vector x and two parameters θ, θ'. If $t \in [0,1] \mapsto \theta(t)$ is an x-admissible trajectory between θ and θ' then*

$$|R_\theta(x) - R_{\theta'}(x)| \leqslant \|x\|_\infty \|\Phi^I(\theta) - \Phi^I(\theta')\|_1 + \|\Phi^H(\theta) - \Phi^H(\theta')\|_1. \tag{17}$$

Proof. In this proof, we denote by convention $x_u := 1$ for any u that is not an input neuron. Recall that p_0 denotes the first neuron of a path p, and x_{p_0} is the coordinate of x for neuron p_0. Since for every parameters θ and every input x, it holds [Gonon et al., 2024, Lemma A.1]

$$R_\theta(x) = \sum_{p \in \mathcal{P}} x_{p_0} a_p(\theta, x) \Phi_p(\theta),$$

we deduce that for every $k \in \{1, \dots, m\}$ and every $t_{k-1} < t' < t < t_k$, we have:

$$R_{\theta(t)}(x) - R_{\theta(t')}(x) = \sum_{p \in \mathcal{P}} x_{p_0} \left(a_p(\theta(t), x) \Phi_p(\theta(t)) - a_p(\theta(t'), x) \Phi_p(\theta(t')) \right).$$

Since both t and t' belong to the same interval (t_{k-1}, t_k) and since $t \mapsto \theta(t)$ is an admissible trajectory, the path-activations $a_p(\theta(t), x) = a_p(\theta(t'), x)$ are the same for every path p. Thus, it holds:

$$R_{\theta(t)}(x) - R_{\theta(t')}(x) = \sum_{p \in \mathcal{P}} x_{p_0} a_p(\theta(t), x) \left(\Phi_p(\theta(t)) - \Phi_p(\theta(t')) \right).$$

Recall that the set of paths $\mathcal{P}$ is partitioned into the sets $\mathcal{P}_I$ and $\mathcal{P}_H$ of paths starting respectively from an input and a hidden neuron. By the convention taken in this proof, for $p \in \mathcal{P}_H$, it holds $x_{p_0} = 1$. Thus:

$$R_{\theta(t)}(x) - R_{\theta(t')}(x) = \sum_{p \in \mathcal{P}_I} x_{p_0} a_p(\theta(t), x) \left(\Phi_p(\theta(t)) - \Phi_p(\theta(t')) \right) + \sum_{p \in \mathcal{P}_H} a_p(\theta(t), x) \left(\Phi_p(\theta(t)) - \Phi_p(\theta(t')) \right).$$

Recall that a path-activation is always equal to 0 or 1 by definition, so that:

$$\begin{aligned} \left| R_{\theta(t)}(x) - R_{\theta(t')}(x) \right| &\leqslant \sum_{p \in \mathcal{P}_I} |x_{p_0}| \, |\Phi_p(\theta(t)) - \Phi_p(\theta(t'))| + \sum_{p \in \mathcal{P}_H} |\Phi_p(\theta(t)) - \Phi_p(\theta(t'))| \\ &\leqslant \|x\|_\infty \|\Phi^I(\theta(t)) - \Phi^I(\theta(t'))\|_1 + \|\Phi^H(\theta(t)) - \Phi^H(\theta(t'))\|_1. \end{aligned}$$

[6] While the standard terminology for such a map $t \mapsto \theta(t)$ is rather "path" than "trajectory", we chose "trajectory" to avoid possible confusions with the notion of "path" of a DAG associated with a neural network.

Considering the limits $t \to t_k$ and $t' \to t_{k-1}$ gives by continuity of both $\theta \mapsto R_\theta(x)$ and $\theta \mapsto \Phi(\theta)$:

$$\left|R_{\theta_k}(x) - R_{\theta_{k-1}}(x)\right| \leqslant \|x\|_\infty \|\Phi^I(\theta_k) - \Phi^I(\theta_{k-1})\|_1 + \|\Phi^H(\theta_k) - \Phi^H(\theta_{k-1})\|_1.$$

Since $\theta = \theta_0$ and $\theta' = \theta_m$, using the triangle inequality yields:

$$|R_\theta(x) - R_{\theta'}(x)| \leqslant \|x\|_\infty \sum_{k=1}^{m} \|\Phi^I(\theta_k) - \Phi^I(\theta_{k-1})\|_1 + \sum_{k=1}^{m} \|\Phi^H(\theta_k) - \Phi^H(\theta_{k-1})\|_1. \tag{18}$$

See Figure 3 for an illustration of what is happening here. By definition, since the trajectory is x-admissible, we have by Inequality (16)

$$\sum_{k=1}^{m} \|\Phi^I(\theta_k) - \Phi^I(\theta_{k-1})\|_1 \leqslant \|\Phi^I(\theta_m) - \Phi^I(\theta_0)\|_1 = \|\Phi^I(\theta') - \Phi^I(\theta)\|_1$$

and

$$\sum_{k=1}^{m} \|\Phi^H(\theta_k) - \Phi^H(\theta_{k-1})\|_1 \leqslant \|\Phi^H(\theta_m) - \Phi^H(\theta_0)\|_1 = \|\Phi^H(\theta') - \Phi^H(\theta)\|_1.$$

With Inequality (18), this proves Inequality (17). □

Construction of an admissible trajectory. In the formal proof of Theorem B.1 we will see that it is enough to establish the result when all the coordinates of θ, θ' are nonzero.

Definition B.4. Consider two parameters θ, θ' with only nonzero coordinates. For every $t \in [0,1]$ and every i, define the following trajectory[7] $t \mapsto \theta(t)$ between θ and θ':

$$(\theta(t))_i = \operatorname{sgn}(\theta_i)|\theta_i|^{1-t}|\theta'_i|^t, \tag{19}$$

where $\operatorname{sgn}(y) := \mathbb{1}_{y>0} - \mathbb{1}_{y<0} \in \{-1, 0, +1\}$ for any $y \in \mathbb{R}$.

Observe that the trajectory in Equation (19) is well-defined since the coordinates of θ and θ' are nonzero by assumption. As proved in the next lemma, this trajectory has indeed finitely many breakpoints where the path-activations change. This is basically because for every coordinate i, the trajectory $t \in [0,1] \to (\theta(t))_i$ is analytic[8]. As a consequence, the set of t's where a coordinate of the path-activations matrix $\boldsymbol{A}(\theta(t), x)$ does change can be realized as a set of zeroes of an analytic function on $\mathbb{C}$, and since these zeroes must be isolated, there could only be finitely of them in the compact $[0,1]$, except when the set of zeroes is the whole $[0,1]$.

Lemma B.5. *Consider $n \in \mathbb{N}_{>0}$ inputs $X = (x_1, \dots, x_n) \in (\mathbb{R}^{d_{in}})^n$. For parameters θ, θ' with only nonzero coordinates, consider the trajectory $t \in [0,1] \mapsto \theta(t)$ defined in Equation (19). There exists finitely many breakpoints $0 = t_0 < t_1 < \cdots < t_m = 1$ such that for every $i = 1, \dots, n$, the path-activations matrix $t \in [0,1] \mapsto \boldsymbol{A}(\theta(t), x_i)$ is constant on each interval (t_k, t_{k+1}).*

Proof of Lemma B.5. After showing that the result for arbitrary n follows from the result for $n = 1$, we establish the latter by an induction on a topological sorting of the graph G.

Reduction to $n = 1$. If for every $i = 1, \dots, n$, we have a finite family of breakpoints $(t_k^i)_k$, then the union of these families gives a finite family of breakpoints that works for every i. It is then sufficient to prove that for a *single* arbitrary input x, there are finitely many breakpoints $0 = t_0 < t_1 < \cdots < t_m = 1$ such that the path-activations matrix $t \in [0,1] \mapsto \boldsymbol{A}(\theta(t), x)$ remains constant on each interval (t_k, t_{k+1}).

For the rest of the proof, consider a single input x, and define for any neuron v the property

$$\begin{gathered}\text{there are finitely many breakpoints } 0 = t_0 < t_1 < \cdots < t_m = 1 \text{ such that for every } k: \\ \text{the map } t \in [t_k, t_{k+1}] \mapsto v(\theta(t), x) \text{ is analytic,} \\ \text{and the functions } t \mapsto a_v(\theta(t), x), t \mapsto a_{u \to v}(\theta(t), x), \text{for each } u \in \operatorname{ant}(v), \text{are constant on } (t_k, t_{k+1})\end{gathered} \tag{20}$$

[7] This trajectory is linear in log-parameterization: for every i, the map $t \mapsto \ln(|(\theta(t))_i|)$ is linear in t.

[8] A function $f : C \mapsto \mathbb{R}$ is analytic on a *closed* subset $C \subset \mathbb{R}$ if there exists an open set $C \subset O \subset \mathbb{R}$ such that f is the restriction to C of a function that is analytic on O.

Reduction to proving Property (20) for every neuron v. We will soon prove that Property (20) holds for every neuron v. Let us see why this is enough to reach the desired conclusion. By the same argument as in the reduction to $n = 1$, the union of the breakpoints associated to all neurons yields finitely many intervals such that, on each interval, *all functions* $t \mapsto a_v(\theta(t), x)$, $v \in N$, and $a_{u\to v}(\theta(t), x)$, $u \in \mathrm{ant}(v)$, are constant. By Definition A.5 this implies that $t \mapsto \boldsymbol{A}(\theta(t), x)$ is constant on each corresponding open interval.

Proof of Property (20) for every neuron v by induction on a topological sorting [Cormen et al., 2009, Section 22.4] of the graph. We start with input neurons v since by Definition A.2, these are the ones without antecedents so they are the first to appear in a topological sorting.

Initialization: Property (20) for input neurons. For any input neuron v, it holds by Definition A.2 $v(\theta, x) = x_v$ that is constant in θ. Thus $t \in [0, 1] \mapsto v(\theta(t), x)$ is trivially analytic. Since v is an input neuron, it has no antecedent, and by Definition A.5 we have $a_v(\theta, x) := 1$. This shows that Property (20) holds for input neurons.

Induction: Now, consider a non-input neuron v and assume Property (20) to hold for every neuron coming before v in the considered topological sorting. Since every antecedent of v must come before v in the topological sorting, there are finitely many breakpoints $0 = t_0 < t_1 < \cdots < t_m = 1$ such that for every $u \in \mathrm{ant}(v)$ and every k, the map $t \in [t_k, t_{k+1}] \mapsto u(\theta(t), x)$ is analytic. We distinguish three cases depending on the activation function of neuron v.

- **Case of an identity neuron.** By Definition A.2 $v(\theta(t), x) = b_v + \sum_{u\in\mathrm{ant}(v)} u(\theta(t), x)\theta(t)^{u\to v}$ and for every k it is clear that it is analytic as it is the case for each $t \in [t_k, t_{k+1}] \mapsto u(\theta(t), x)$ by induction, and it is also the case for $t \in [t_k, t_{k+1}] \mapsto \theta(t)^{u\to v}$ by definition (Equation (19)). Since v is an identity neuron by Definition A.5 we have $a_{u\to v}(\theta(t), x) = a_v(\theta(t), x) = 1$ for every t. This establishes Property (20) for v.
- **Case of a ReLU neuron.** By Definition A.2: $v(\theta, x) = \mathrm{ReLU}(\mathrm{pre}_v(\theta, x))$ where we denote the so-called pre-activation of v by $\mathrm{pre}_v(\theta, x) := b_v + \sum_{u\in\mathrm{ant}(v)} u(\theta, x)\theta^{u\to v}$. Reasoning as in the case of identity neurons, the induction hypothesis implies that for every k the function $t \in [t_k, t_{k+1}] \mapsto \mathrm{pre}_v(\theta(t), x)$ is analytic. We distinguish two sub-cases:

  – If this function is identically zero then $t \in [t_k, t_{k+1}] \mapsto v(\theta(t), x)$ is null, so it is analytic, and by Definition A.5 $a_{u\to v}(\theta(t), x) = a_v(\theta(t), x) = \mathbb{1}_{v(\theta,x)>0} = 0$ for every $u \in \mathrm{ant}(v)$;

  – Otherwise this analytic function can only vanish a finite number of times on the compact $[t_k, t_{k+1}]$: there are times $t_k = s_0 < s_1 < \cdots < s_n = t_{k+1}$ such that for each j, $s \in (s_j, s_{j+1}) \mapsto \mathrm{pre}_v(\theta(s), x)$ has constant (nonzero) sign and can be extended into an analytic function on $\mathbb{C}$. For each segment (s_j, s_{j+1}) where the sign is negative, we deduce that for every $s \in [s_j, s_{j+1}]$ we have $v(\theta(s), x) = 0$, hence by Definition A.5, $a_v(\theta(s), x) = a_{u\to v}(\theta(s), x) = 0$ for every $u \in \mathrm{ant}(v)$; on the other segments, we have $v(\theta(s), x) = \mathrm{pre}_v(\theta(s), x)$ for every $s \in [s_j, s_{j+1}]$, and therefore $a_v(\theta(s), x) = a_{u\to v}(\theta(s), x) = 1$ for every $s \in (s_j, s_{j+1})$ and $u \in \mathrm{ant}(v)$. Overall, on all the resulting (finitely many) segments, we obtain all the properties establishing that Property (20) indeed holds for v.
- **Case of a K-max-pooling neuron.** Recall that by Definition A.2, the output of v is the K-th largest component of $\mathrm{pre}_v(\theta, x) := (u(\theta, x)\theta^{u\to v})_{u\in\mathrm{ant}(v)}$, with ties between antecedents decided by lexicographic order. Since each $t \in [t_k, t_{k+1}] \mapsto u(\theta(t), x)$ is analytic, and so does $t \mapsto \theta(t)^{u\to v}$, this is also the case of each coordinate of $\mathrm{pre}_v(\theta(t), x)$.

  Consider any k. We are going to prove that there are finitely many breakpoints $t_k = s_0 < s_1 < \cdots < s_\ell = t_{k+1}$ such that on each interval (s_j, s_{j+1}), there is an antecedent $u \in \mathrm{ant}(v)$ such that

$$v(\theta(s), x) = u(\theta(s), x)\theta(s)^{u\to v}, \text{ for every } s \in (s_j, s_{j+1}).$$

  By the same reasoning as above this will imply that Property (20) holds for v.

  For any neurons $u \neq u' \in \mathrm{ant}(v)$, denote $\delta_{u,u'}(\theta) := u(\theta(t), x)\theta(t)^{u\to v} - u'(\theta(t), x)\theta(t)^{u'\to v}$ and let U be the set of $u \in \mathrm{ant}(v)$ such that: for each $u' \in \mathrm{ant}(v)$, either $t \mapsto \delta_{u,u'}(\theta(t))$ is not identically zero on $[t_k, t_{k+1}]$, or u is before u' in lexicographic order. With this definition, for each pair $u \neq u' \in U$, the function $t \in [t_k, t_{k+1}] \mapsto \delta_{u,u'}(\theta(t), x)$ is not identically zero and is analytic, so that there are only finitely many breakpoints $t_k = s_0^{u,u'} < s_1^{u,u'} < \cdots < s_{\ell(u,u')}^{u,u'} = t_{k+1}$ where it vanishes on the compact $[t_k, t_{k+1}]$. Considering the union over all pairs $u, u' \in U$ of these finite families of breakpoints, we get a finite family of breakpoint $t_k = s_0 < s_1 < \cdots < s_\ell = t_{k+1}$ such that on each interval (s_j, s_{j+1}), the ordering between the coordinates of $\mathrm{pre}_v(\theta(s), x)$ in U is strict and stays the same. To conclude, it is not hard to check that, by the definition of U and of $*$-max-pooling, the output of v only depends on the coordinates of $\mathrm{pre}_v(\theta(s), x)$ indexed by U. This

yields the claim and concludes the proof. □

For $y \in \mathbb{R}$, recall that we consider $\operatorname{sgn}(y) = \mathbb{1}_{y>0} - \mathbb{1}_{y<0} \in \{-1, 0, +1\}$ and extend it to vectors by applying it coordinate-wise.

Corollary B.6. *Consider two parameters θ, θ' with nonzero coordinates and such that $\operatorname{sgn}(\theta) = \operatorname{sgn}(\theta')$. Then the trajectory defined in Equation (19) is x-admissible for every input vector x.*

Proof. First, the trajectory is well-defined since the coordinates are nonzero, and it satisfies the boundary conditions $\theta(0) = \theta$ and $\theta(1) = \theta'$ since the coordinates have the same signs.

Second, Lemma B.5 proves that for every x, there are finitely many breakpoints $0 = t_0 < t_1 < \cdots < t_m = 1$ such that the path-activations matrix $t \in [0,1] \mapsto \boldsymbol{A}(\theta(t), x)$ is constant on each interval (t_{k-1}, t_k).

It now only remains to prove that Inequality (16) holds to prove that this is an x-admissible trajectory. Consider a path p. For a coordinate i of the parameters, we write $i \in p$ either if $i = p_0$ and p_0 is a hidden neuron, or if $i = e$ is an edge along the path p. Define $\operatorname{sgn}(p) := \prod_{i \in p} \operatorname{sgn}(\theta_i)$ and note that $\operatorname{sgn}(p) \neq 0$ since θ has only nonzero coordinates by assumption. Denote $|\theta|$ the vector deduced from θ by applying the absolute value coordinate-wise. It is easy to check by definition of the path-lifting Φ that for every $t \in [0,1]$:

$$\Phi_p(\theta(t)) = \operatorname{sgn}(p)\Phi_p(|\theta|)^{1-t}\Phi_p(|\theta'|)^t = \operatorname{sgn}(p)\Phi_p(|\theta(t_0)|)^{1-t}\Phi_p(|\theta(t_m)|)^t.$$

Denote by $a := \Phi_p(|\theta'|) = \Phi_p(|\theta(t_m)|)$ and by $b = \Phi_p(|\theta|) = \Phi_p(|\theta(t_0)|)$. The latter rewrites:

$$\Phi_p(\theta(t)) = \operatorname{sgn}(p) a^t b^{1-t}.$$

Thus, Inequality (16) holds if, and only if,

$$\sum_{k=1}^{m} |\operatorname{sgn}(p)| \left| a^{t_k} b^{1-t_k} - a^{t_{k-1}} b^{1-t_{k-1}} \right| \leqslant |\operatorname{sgn}(p)| \, |a - b| \, .$$

Simplifying by $\operatorname{sgn}(p) \neq 0$, Inequality (16) is equivalent to:

$$\sum_{k=1}^{m} \left| a^{t_k} b^{1-t_k} - a^{t_{k-1}} b^{1-t_{k-1}} \right| \leqslant |a - b| \, .$$

Let us now observe that $t \mapsto a^t b^{1-t}$ is monotonic and conclude. We only do so when $a \geqslant b$, the other case being similar. Since by definition, we also have a and b positive, it holds for $t > t'$

$$a^{t-t'} \geqslant b^{t-t'} \text{ that is equivalent to } a^t b^{1-t'} \geqslant a^t b^{1-t'} .$$

We then have a telescopic sum:

$$\sum_{k=1}^{m} \left| a^{t_k} b^{1-t_k} - a^{t_{k-1}} b^{1-t_{k-1}} \right| = \sum_{k=1}^{m} a^{t_k} b^{1-t_k} - a^{t_{k-1}} b^{1-t_{k-1}} = a^{t_m} b^{1-t_m} - a^{t_0} b^{1-t_0} = a - b = |a - b| \, .$$

This shows Inequality (16), proving that $t \mapsto \theta(t)$ is an admissible trajectory, and thus the result. □

Proof of Theorem B.1. **Equality case.** Consider an arbitrary neural network architecture, an input neuron v_0 and a path $p = v_0 \to v_1 \to \dots v_d$. Consider θ (resp. θ') with only zero coordinates, except for $\theta^{v_\ell \to v_{\ell+1}} = a > 0$ (resp. $(\theta')^{v_\ell \to v_{\ell+1}} = b > 0$) for every $\ell \in [\![0, d-1]\!]$. Consider the input x to have only zero coordinates except for $x_{v_0} > 0$. It is easy to check that $R_\theta(x) = a^d x_{v_0}$ and $R_{\theta'}(x) = b^d x_{v_0}$. Since $\|x\|_\infty = x_{v_0}$, $\|\Phi^I(\theta) - \Phi^I(\theta')\|_1 = |a^d - b^d|$ and $\|\Phi^H(\theta) - \Phi^H(\theta')\|_1 = 0$, this shows that Inequality (15) is an equality for these parameters.

Proof of the inequality. By continuity of both handsides of (15) with respect to θ, θ', it is enough to prove the result when all coordinates of θ, θ' are nonzero, i.e., under the stronger assumption that $\theta_i \theta'_i > 0$ for every coordinate index i. Under this assumption, by Corollary B.6, the trajectory $t \mapsto \theta(t)$ defined in Equation (19) is x-admissible for every input vector x. The conclusion follows by Lemma B.3. □

C Proof of Lemma 4.2

Rescaling-invariance is a direct consequence of the known properties of the path-lifting Φ Gonon et al. [2024].

In the case of a singleton $I = \{i\}$, as already evoked, (13) simply follows from (5) and the definition of `Path-Mag`. When $|I| \geqslant 2$, consider any enumeration i_j, $1 \leqslant j \leqslant |I|$ of elements in I, and $s_j := \mathbf{1}_G - \sum_{\ell=1}^{j} e_{i_\ell} = \mathbf{1}_G - \mathbf{1}_{\cup_{\ell=1}^{j}\{i_\ell\}}$ (as well as $s_0 := \mathbf{1}_G$): since the pair $(\theta, s \odot \theta)$ –as well as the pairs $(s_{j-1} \odot \theta, s_j \odot \theta)$– satisfies the assumptions of Lemma 3.2, and $s_j \odot s_{j-1} = s_j$ we have

$$\begin{aligned}
\|\Phi(\theta) - \Phi(s \odot \theta)\|_1 &\underset{(7)}{=} \|\Phi(\theta)\|_1 - \|\Phi(s \odot \theta)\|_1 \\
&= \sum_{j=1}^{|I|} \|\Phi(s_{j-1} \odot \theta)\|_1 - \|\Phi(s_j \odot \theta)\|_1 \\
&\underset{(7)}{=} \sum_{j=1}^{|I|} \|\Phi(s_{j-1} \odot \theta) - \Phi(s_j \odot (s_{j-1} \odot \theta))\|_1 \\
&\underset{(10)}{=} \sum_{j=1}^{|I|} \texttt{Path-Mag}(s_{j-1} \odot \theta, i_j) \\
&\underset{(12)}{\leqslant} \sum_{j=1}^{|I|} \texttt{Path-Mag}(\theta, i_j).
\end{aligned}$$

Finally, to establish (14), observe that for each path p we have $|\Phi_p(\theta)| = \prod_{j \in p} |\theta_j|$ so, for each $i \in p$ (NB: i can index either an edge in the path or the first neuron of p when p starts from a hidden or output neuron, in which case θ_i is the associated bias) it holds

$$\frac{\partial}{\partial \theta_i} |\Phi_p(\theta)| = \operatorname{sgn}(\theta_i) \prod_{j \in p, j \neq i} |\theta_j|.$$

Because $\operatorname{sgn}(\theta_i)\theta_i = |\theta_i|$ we get that, when $i \in p$,

$$\theta_i \cdot \frac{\partial}{\partial \theta_i} |\Phi_p(\theta)| = |\Phi_p(\theta)|.$$

Summing over all paths for a given index i shows that

$$\begin{aligned}
(\theta \odot \nabla_\theta \|\Phi(\theta)\|_1)_i &= \theta_i \frac{\partial}{\partial \theta_i} \sum_{p \in \mathcal{P}} |\Phi_p(\theta)| \\
&= \theta_i \sum_{p \in \mathcal{P} : i \in p} \frac{\partial}{\partial \theta_i} |\Phi_p(\theta)| \\
&= \sum_{p \in \mathcal{P} : i \in p} |\Phi_p(\theta)| \\
&\underset{(12)}{=} \texttt{Path-Mag}(\theta, i).
\end{aligned}$$

D Proof-of-concept: accuracy of path-magnitude pruning

To provide a proof-of-concept of the utility of the main Lipschitz bound in Theorem 3.1 for pruning, we implement the following "prune and finetune" procedure:

1. **train**: we train a dense network,
2. **rescale (optional)**: we apply a random rescale to the trained weights (this includes biases),

3. **prune**: we prune the resulting network,

4. **rewind**: we rewind the weights to their value after a few initial epochs (standard in the lottery ticket literature to enhance performance [Frankle et al., 2020]),

5. **finetune**: we retrain the pruned network, with the pruned weights frozen to zero and the other ones initialized from their rewinded values.

Doing that to prune $p = 40\%$ of the weights at once of a ResNet18 trained on ImageNet-1k, we observe that (Figure 6):

- **without random rescale** (plain lines), the test accuracy obtained at the end is *similar* for both magnitude pruning and path-magnitude pruning;

- **with random rescale** (dotted lines – the one associated with path-magnitude pruning is invisible as it coincides with the corresponding plain line), magnitude pruning suffers a large drop of top-1 test accuracy, which is not the case of path-magnitude pruning since it makes the process invariant to potential rescaling.

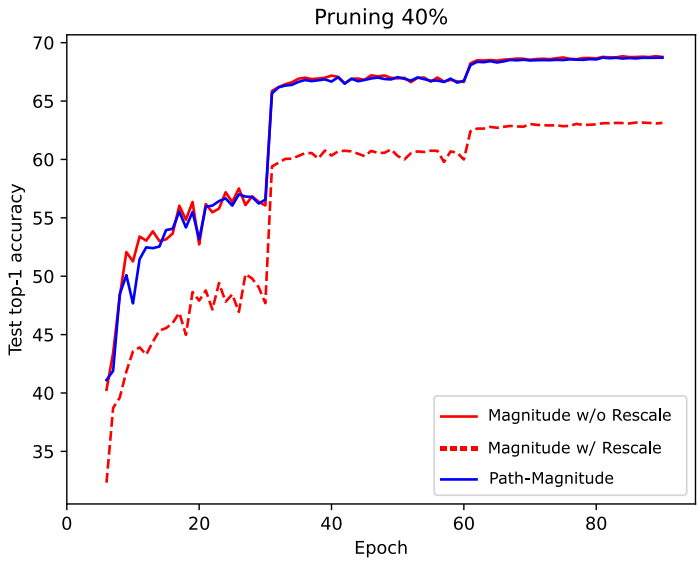

Figure 6: Training Curves: Test Top-1 Accuracy resulting from the different variants of the "prune and finetune" procedure, with (dashed line) or without (plain line) random rescaling of the initially trained weights. The results for path-magnitude pruning are the same with or without rescaling, hence the corresponding dashed line (random rescale applied beforehand) *is invisible*, as it perfectly overlaps with the plain line (no rescale), unlike for magnitude pruning. Accuracy jumps around epochs 30 and 60 corresponding to change in learning rate.

We observe similar results when pruning between $p = 10\%$ and $p = 80\%$ of the weights at once, see Table 4.

We now give details on each stage of the procedure.

1. Train. We train a dense ResNet18 [He et al., 2016] on ImageNet-1k, using 99% of the 1,281,167 images of the training set for training, the other 1% for validation. We use SGD for 90 epochs, learning rate 0.1, weight-decay 0.0001, batch size 1024, classical ImageNet data normalization, and a multi-step scheduler where the learning rate is divided by 10 at epochs 30, 60 and 80. The epoch out of the 90 ones with maximum validation top-1 accuracy is considered as the final epoch. Doing 90 epochs took us about 18 hours on a single A100-40GB GPU.

Table 4: Top-1 accuracy after pruning, optional rescale, rewind and retrain, as a function of the pruning level. $(*)$ = results valid with as well as without rescaling, as path-magnitude pruning is invariant to rescaling.

Pruning level	none	10%	20%	40%	60%	80%
Path-Magnitude $(*)$	67.7%	68.6	68.8	68.6	67.9	66.0
Magnitude w/o Random Rescale		69.0	69.0	68.8	68.2	66.5
Magnitude w/ Random Rescale		68.8	68.7	63.1	57.5	15.8

2. Random rescaling. Consider a pair of consecutive convolutional layers in the same basic block of the ResNet18 architecture, for instance the ones of the first basic block: `model.layer1[0].conv1` and `model.layer1[0].conv2` in PyTorch, with `model` being the ResNet18. Denote by C the number of output channels of the first convolutional layer, which is also the number of input channels of the second one. For each channel $c \in [\![1, C]\!]$, we choose uniformly at random a rescaling factor $\lambda \in \{1, 128, 4096\}$ and multiply the output channel c of the first convolutional layer by λ, and divide the input channel c of the second convolutional layer by λ. In order to preserve the input-output relationship, we also multiply by λ the running mean and the bias of the batch normalization layer that is in between (`model.layer1[0].bn1` in the previous example). Here is an illustrative Python code (that should be applied to the correct layer weights as described above):

```
    factors = np.array([1, 128, 4096])

    out_channels1, _, _, _ = weights_conv1.shape

    for out in range(out_channels1):
                factor = np.random.choice(factors)
                weights_conv1[out, :, :, :] *= factor
                weights_conv2[:, out, :, :] /= factor
                running_mean[out] *= factor
                bias[out] *= factor
```

3. Pruning. At the end of the training phase, we globally prune (i.e. set to zero) $p\%$ of the remaining weights in all the convolutional layers plus the final fully connected layer.

4. Rewinding. We save the mask and rewind the weights to their values after the first 5 epochs of the dense network, and train for 85 remaining epochs. This exactly corresponds to the hyperparameters and pruning algorithm of the lottery ticket literature [Frankle et al., 2021].

5. Finetune. This is done in the same conditions as the training phase.

E Computational cost: comparing pruning criteria

This section details how the results of Table 3 were obtained.

E.1 Hardware and software

All experiments were performed on an NVIDIA A100-PCIE-40GB GPU, with CPU Intel(R) Xeon(R) Silver 4215R CPU @ 3.20GHz. We used `PyTorch` (version *2.2*, with `CUDA` *12.1* and `cuDNN` *8.9* enabled) to implement model loading, inference, and custom pruning-cost computation. All timings were taken using the `torch.utils.benchmark` module, synchronizing the GPU to ensure accurate measurement of wall-clock time.

E.2 Benchmarked code

Single-forward pass. We fed a tensor torch.randn(B, 3, 224, 224) to each model (batch size $B = 1$ or $B = 128$, 224×224 RGB image).

Path-magnitude scores. We followed the recipe given in (14): $(\texttt{Path-Mag}(\theta, i))_i = \theta \odot \nabla_\theta \|\Phi(\theta)\|_1$. To do that, we computed the path-norm $\|\Phi(\theta)\|_1$ using the function `get_path_norm` we released online at `github.com/agonon/pathnorm_toolkit`. And we simply added one line to auto-differentiate the computations and multiply the result pointwise with the parameters θ. Thus, our code has the following structure:

- it starts by replacing max-pooling *neurons* by summation *neurons*, or equivalently max-pooling *layers* by convolutional *layers* (following the recipe given in Gonon et al. [2024] to compute correctly the path-norm),
- it replaces each weight by its absolute value,
- it does a forward pass to compute the path-norm,
- here we added auto-differentiation (backwarding the path-norm computations), and pointwise multiplication with original weights,
- and it finally reverts to the original maxpool layers and the weights' value to restore the original network.

Table 3 reports the time to do all this.

Magnitude scores. It takes as input a torch model, and does a simple loop over all model's parameters:

- to check if these are the parameters of a `torch.nn.Linear` or `torch.nn.Conv2d` module,
- if this is the case, it adds to a list the absolute values of these weights.

Loss-sensitivity scores LeCun et al. [1989]. In the Optimal Brain Damage (OBD) framework introduced in LeCun et al. [1989], each weight θ_i in the network is assigned a score approximating the expected increase in loss if θ_i were pruned (set to zero). The score of θ_i is defined by:

$$\text{OBD}(\theta, i) = \frac{1}{2} h_{ii} \theta_i^2,$$

where h_{ii} is the diagonal entry of the Hessian matrix $H = \nabla^2 \ell$ of the empirical loss

$$\ell(\theta) = \sum_{k=1}^{n} \ell(R_\theta(x_k), y_k)$$

with respect to the parameters θ. As we could not locate a proof of the rescaling-invariance of OBD we give below a short proof, before discussing its numerical computation.

Rescaling-invariance. Denote $D = \texttt{diag}(\lambda_i)$ a diagonal rescaling matrix such that for each θ the parameters $\theta' := D\theta$ are rescaling-equivalent to θ. This implies that $R_\theta(x_k) = R_{D\theta}(x_k)$ for each training sample x_k and every θ, hence $\ell(\theta) = \ell(D\theta)$ for every θ. Simple calculus then yields equality of the Jacobians $\partial \ell(\theta) = \partial \ell(D\theta) D$, i.e., since D is symmetric, taking the transpose

$$\nabla \ell(\theta) = D \nabla \ell(D\theta), \quad \forall \theta,$$

that is to say $\nabla \ell(\cdot) = D \nabla \ell(D\cdot)$. Differentiating once more yields

$$H(\theta) = \nabla^2 \ell(\theta) = \partial[\nabla \ell](\theta) = \partial[D \nabla \ell(D\cdot)](\theta) = D \partial[\nabla \ell(D\cdot)](\theta) = D \partial[\nabla \ell(\cdot)](D\theta) D = D H(D\theta) D.$$

Extracting the i-th diagonal entry yields $h_{ii}(\theta) = \lambda_i^2 h_{ii}(D\theta)$ (and more generally $h_{ij}(\theta) = \lambda_i \lambda_j h_{ij}(D\theta)$), hence

$$\text{OBD}(D\theta, i) = \frac{1}{2} h_{ii}(D\theta)((D\theta)_i)^2 = \frac{1}{2} h_{ii}(D\theta)(\lambda_i \theta_i)^2 = \frac{1}{2}[h_{ii}(D\theta)\lambda_i^2]\theta_i^2 = \frac{1}{2} h_{ii}(\theta)\theta_i^2 = \text{OBD}(\theta, i). \tag{21}$$

Computation. Computing the full Hessian matrix H exactly would be prohibitive for large networks. Instead, a well-known variant of Hutchinson's trick Bekas et al. [2007] is that its diagonal can be computed as

$$\operatorname{diag}(H) = \mathbb{E}_v\big[(Hv) \odot v\big]$$

where the expectation is over Rademacher vectors v (i.i.d. uniform $v_i \in \{-1, 1\}$) and where $\odot$ denotes pointwise multiplication. In practice, we approximate it as follows:

- draw a *single vector* v as above,
- compute the Hessian-vector product Hv using the "reverse-over-forward" higher-order autodiff in PyTorch's `torch.func` API,
- deduce the estimate $\operatorname{diag}(H) \simeq (Hv) \odot v =: u$,
- finally estimate OBD $\simeq \frac{1}{2} u \odot \theta \odot \theta = \frac{1}{2}(Hv) \odot v \odot \theta \odot \theta$.

The performance to do all this depends on the size of the batch on which is computed the loss, as the cost of the Hessian-vector product Hv depends on it. Table 3 reports the milliseconds required for this entire procedure on batch sizes of 1 and 128, listing corresponding values as $x - y$.

This approximation is *not* rescaling-invariant in general. Indeed, we have

$$\begin{aligned}((Hv) \odot v \odot \theta \odot \theta)_i = (Hv)_i \cdot v_i \cdot \theta_i^2 &= \left(\sum_j h_{ij}(\theta) v_j\right) v_i \theta_i^2 \\ &\underset{(21)}{=} \left(\sum_j \lambda_i \lambda_j h_{ij}(D\theta) v_j\right) v_i \theta_i^2 = \left(\sum_j \lambda_j h_{ij}(D\theta) v_j\right) v_i \lambda_i \theta_i^2\end{aligned}$$

which would be the same as the estimate made for $D\theta$ if and only if it were equal to

$$\left(\sum_j h_{ij}(D\theta) v_j\right) v_i \lambda_i^2 \theta_i^2.$$

There is no reason for this to happen (and it did not happen in any of our experiments). For instance, take $v_i = \theta_i = 1$ for every i, we would need $\sum_j \lambda_j h_{ij}(D\theta) = \lambda_i \sum_j h_{ij}(D\theta)$, which is the same as saying that λ is an eigenvector of $H(D\theta)$ with eigenvalue 1.

F Lipschitz property of Φ: proof of Lemma 3.3

We first establish Lipschitz properties of $\theta \mapsto \Phi(\theta)$. Combined with the main result of this paper, Theorem 3.1, or with Corollary B.2, they establish a Lipschitz property of $\theta \mapsto R_\theta(x)$ for each x, and of the functional map $\theta \mapsto R_\theta(\cdot)$ in the uniform norm on any bounded domain. This is complementary to the Lipschitz property of $x \mapsto R_\theta(x)$ studied elsewhere in the literature, see e.g. [Gonon et al., 2024].

Lemma F.1. *Consider $q \in [1, \infty)$, parameters θ and θ', and a neuron v. Then, it holds:*

$$\begin{aligned}&\|\Phi^{\to v}(\theta) - \Phi^{\to v}(\theta')\|_q^q \\ &\leqslant \max_{p \in \mathcal{P}^{\to v}} \sum_{\ell=1}^{\texttt{length}(p)} \left(\prod_{k=\ell+1}^{\texttt{length}(p)} \|\theta^{\to p_k}\|_q^q\right) \left(|b_{p_\ell} - b'_{p_\ell}|^q + \|\theta^{\to p_\ell} - (\theta')^{\to p_\ell}\|_q^q \max_{u \in \operatorname{ant}(p_\ell)} \|\Phi^{\to u}(\theta')\|_q^q\right)\end{aligned} \tag{22}$$

with the convention that an empty sum and product are respectively equal to zero and one. Recall also that by convention, biases of $*$-max-pooling neurons v are set to $b_v = 0$ (Definition A.5).

Note that when all the paths in $\mathcal{P}^{\to v}$ have the same length L, Inequality (22) is homogeneous: multiplying both θ and θ' coordinate-wise by a scalar λ scales both sides of the equations by λ^L.

Proof. The proof of Inequality (22) goes by induction on a topological sorting of the graph. The first neurons of the sorting are the neurons without antecedents, *i.e.*, the input neurons by definition. Consider an input neuron v. There is only a single path ending at v: the path $p = v$. By Definition A.5, $\Phi^{\to v}(\cdot) = \Phi_v(\cdot) = 1$ so the left hand-side is zero. On the right-hand side, there is only a single choice for a path ending at v: this is the path $p = v$ that starts and ends at v. Thus $D = 0$, and the maximum is zero (empty sum). This proves Inequality (22) for input neurons.

Consider a neuron $v \notin N_{\text{in}}$ and assume that this is true for every neuron before v in the considered topological sorting. Recall that, by definition, $\Phi^{\to v}$ is the path-lifting of $G^{\to v}$ (see Definition A.5). The paths in $G^{\to v}$ are $p = v$, and the paths going through antecedents of v (v has antecedents since it is not an input neuron). So we have $\Phi^{\to v}(\theta) = \begin{pmatrix} (\Phi^{\to u} \times \theta^{u\to v})_{u\in \text{ant}(v)} \\ b_v \end{pmatrix}$, where we again recall that $\Phi^{\to u}(\cdot) = 1$ for input neurons u, and $b_u = 0$ for $*$-max-pooling neurons. Thus, we have:

$$\begin{aligned}
&\|\Phi^{\to v}(\theta) - \Phi^{\to v}(\theta')\|_q^q \\
&= |b_v - b'_v|^q + \sum_{u\in \text{ant}(v)} \|\Phi^{\to u}(\theta) \times \theta^{u\to v} - \Phi^{\to u}(\theta') \times (\theta')^{u\to v}\|_q^q \\
&\leqslant |b_v - b'_v|^q + \sum_{u\in \text{ant}(v)} \left(\|\Phi^{\to u}(\theta) - \Phi^{\to u}(\theta')\|_q^q |\theta^{u\to v}|^q + \|\Phi^{\to u}(\theta')\|_q^q |\theta^{u\to v} - (\theta')^{u\to v}|^q\right) \\
&\leqslant |b_v - b'_v|^q + \|\theta^{\to v}\|_q^q \max_{u\in \text{ant}(v)} \|\Phi^{\to u}(\theta) - \Phi^{\to u}(\theta')\|_q^q + \|\theta^{\to v} - (\theta')^{\to v}\|_q^q \max_{u\in \text{ant}(v)} \|\Phi^{\to u}(\theta')\|_q^q.
\end{aligned}$$

Using the induction hypothesis (Inequality (22)) on the antecedents of v and observing that $p \in \mathcal{P}^{\to v}$ if, and only if there are $u \in \text{ant}(v), r \in \mathcal{P}^{\to u}$ such that $p = r \to v$ gives (we highlight in **blue** the important changes):

$$\begin{aligned}
\|\Phi^{\to v}(\theta) - \Phi^{\to v}(\theta)\|_q^q &\leqslant |b_v - b'_v|^q + \|\theta^{\to v} - (\theta')^{\to v}\|_q^q \max_{u\in \text{ant}(v)} \|\Phi^{\to u}(\theta')\|_q^q \\
+\|\boldsymbol{\theta^{\to v}}\|_{\boldsymbol{q}}^{\boldsymbol{q}} \max_{\boldsymbol{u\in \text{ant}(v)}} \max_{\boldsymbol{r\in\mathcal{P}^{\to u}}} &\sum_{\ell=1}^{\texttt{length}(r)} \left(\prod_{k=\ell+1}^{\texttt{length}(r)} \|\theta^{\to r_k}\|_q^q\right) \left(|b_{r_\ell} - b'_{r_\ell}|^q + \|\theta^{\to r_\ell} - (\theta')^{\to r_\ell}\|_q^q \max_{w\in \text{ant}(r_\ell)} \|\Phi^{\to w}(\theta')\|_q^q\right). \\
&= |b_v - b'_v|^q + \|\theta^{\to v} - (\theta')^{\to v}\|_q^q \max_{u\in \text{ant}(v)} \|\Phi^{\to u}(\theta')\|_q^q \\
+ \max_{\boldsymbol{p\in\mathcal{P}^{\to v}}} &\sum_{\ell=1}^{\texttt{length}(\boldsymbol{p})-1} \left(\prod_{k=\ell+1}^{\texttt{length}(p)} \|\theta^{\to p_k}\|_q^q\right) \left(|b_{p_\ell} - b'_{p_\ell}|^q + \|\theta^{\to p_\ell} - (\theta')^{\to p_\ell}\|_q^q \max_{w\in \text{ant}(p_\ell)} \|\Phi^{\to w}(\theta')\|_q^q\right) \\
= \max_{p\in\mathcal{P}^{\to v}} &\sum_{\ell=1}^{\texttt{length}(\boldsymbol{p})} \left(\prod_{k=\ell+1}^{\texttt{length}(p)} \|\theta^{\to p_k}\|_q^q\right) \left(|b_{p_\ell} - b'_{p_\ell}|^q + \|\theta^{\to p_\ell} - (\theta')^{\to p_\ell}\|_q^q \max_{w\in \text{ant}(p_\ell)} \|\Phi^{\to w}(\theta')\|_q^q\right).
\end{aligned}$$

This proves Inequality (22) for v and concludes the induction. □

In the sequel it will be useful to restrict the analysis to *normalized* parameters, defined as parameters $\tilde{\theta}$ such that $\left\| \begin{pmatrix} \tilde{\theta}^{\to v} \\ \tilde{b}_v \end{pmatrix} \right\|_1 \in \{0, 1\}$ for every $v \in N \setminus (N_{\text{out}} \cup N_{\text{in}})$. Thanks to the rescaling-invariance of ReLU neural network parameterizations, Algorithm 1 in Gonon et al. [2024] allows to rescale *any* parameters θ into a normalized version $\tilde{\theta}$ such that $R_{\tilde{\theta}} = R_\theta$ and $\Phi(\theta) = \Phi(\tilde{\theta})$ [Gonon et al., 2024, Lemma B.2]. This implies the next simpler results for normalized parameters.

Theorem F.2. *Consider $q \in [1, \infty)$. For every normalized parameters θ, θ' obtained as the output of Algorithm 1 in Gonon et al. [2024], it holds:*

$$\begin{aligned}
\|\Phi(\theta) - \Phi(\theta')\|_q^q \leqslant &\sum_{v\in N_{out}\setminus N_{in}} |b_v - b'_v|^q + \|\theta^{\to v} - (\theta')^{\to v}\|_q^q \\
&+ \min\left(\|\Phi(\theta)\|_q^q, \|\Phi(\theta')\|_q^q\right) \max_{p\in\mathcal{P}: p_{\text{end}}\notin N_{in}} \sum_{\ell=1}^{\texttt{length}(p)-1} \left(|b_{p_\ell} - b'_{p_\ell}|^q + \|\theta^{\to p_\ell} - (\theta')^{\to p_\ell}\|_q^q\right). \quad (23)
\end{aligned}$$

where we recall that $b_v = 0$ for $*$-max-pooling neurons v.

Denote by $\mathtt{N}(\theta)$ the normalized version of θ, obtained as the output of Algorithm 1 in Gonon et al. [2024]. It can be checked that if $\theta = \mathtt{N}(\tilde{\theta})$ and $\theta' = \mathtt{N}(\tilde{\theta}')$, and if all the paths have the same lengths L, then multiplying both $\tilde{\theta}$ and $\tilde{\theta}'$ coordinate-wise by a scalar λ does not change their normalized versions θ and θ', except for the biases and the incoming weights of all output neurons that are scaled by λ^L. As a consequence, Inequality (23) is homogeneous: both path-liftings on the left-hand-side and the right-hand-side are multiplied by λ^L, and so is the sum over $v \in N_{\text{out}} \setminus N_{\text{in}}$ in the right-hand-side, while the maximum over p is unchanged since it only involves normalized coordinates that do not change.

For networks used in practice, it holds $N_{\text{out}} \cap N_{\text{in}} = \emptyset$ so that $N_{\text{out}} \setminus N_{\text{in}}$ is just N_{out}, but the above theorem also covers the somewhat pathological case of DAG architectures G where one or more input neurons are also output neurons.

Proof of Theorem F.2. Since $\Phi(\theta) = \left(\Phi^{\to v}(\theta)\right)_{v \in N_{\text{out}}}$, it holds

$$\|\Phi(\theta) - \Phi(\theta')\|_q^q = \sum_{v \in N_{\text{out}}} \|\Phi^{\to v}(\theta) - \Phi^{\to v}(\theta')\|_q^q.$$

By Definition A.5, it holds for every input neuron v: $\Phi^{\to v}(\cdot) = 1$. Thus, the sum can be taken over $v \in N_{\text{out}} \setminus N_{\text{in}}$:

$$\|\Phi(\theta) - \Phi(\theta')\|_q^q = \sum_{v \in N_{\text{out}} \setminus N_{\text{in}}} \|\Phi^{\to v}(\theta) - \Phi^{\to v}(\theta')\|_q^q.$$

Besides, observe that many norms appearing in Inequality (22) are at most one for normalized parameters. Indeed, for such parameters it holds for every $u \in N \setminus (N_{\text{in}} \cup N_{\text{out}})$: $\|\theta^{\to u}\|_q^q \leqslant 1$ [Gonon et al., 2024, Lemma B.2]. As a consequence, for $p \in \mathcal{P}$ and any $\ell \in [\![0, \mathtt{length}(p) - 1]\!]$ we have:

$$\prod_{k=\ell+1}^{\mathtt{length}(p)} \|\theta^{\to p_k}\|_q^q = \left(\prod_{k=\ell+1}^{\mathtt{length}(p)-1} \underbrace{\|\theta^{\to p_k}\|_q^q}_{\leqslant 1} \right) \|\theta^{\to p_{\text{end}}}\|_q^q \leqslant \|\theta^{\to p_{\text{end}}}\|_q^q.$$

Moreover, for normalized parameters θ and $u \notin N_{\text{out}}$, it also holds $\|\Phi^{\to u}(\theta)\|_q^q \leqslant 1$ [Gonon et al., 2024, Lemma B.3]. Thus, Inequality (22) implies for any $v \in N_{\text{out}}$, and any normalized parameters θ and θ':

$$\begin{aligned}
&\|\Phi^{\to v}(\theta) - \Phi^{\to v}(\theta')\|_q^q \\
&\leqslant |b_v - b'_v|^q + \|\theta^{\to v} - (\theta')^{\to v}\|_q^q + \|\theta^{\to v}\|_q^q \max_{p \in \mathcal{P}^{\to v}} \sum_{\ell=1}^{\mathtt{length}(p)-1} \left(|b_{p_\ell} - b'_{p_\ell}|^q + \|\theta^{\to p_\ell} - (\theta')^{\to p_\ell}\|_q^q \right).
\end{aligned}$$

Thus, we get:

$$\begin{aligned}
&\|\Phi(\theta) - \Phi(\theta')\|_q^q \\
&= \sum_{v \in N_{\text{out}} \setminus N_{\text{in}}} \|\Phi^{\to v}(\theta) - \Phi^{\to v}(\theta')\|_q^q \\
&\leqslant \sum_{v \in N_{\text{out}} \setminus N_{\text{in}}} \left(|b_v - b'_v|^q + \|\theta^{\to v} - (\theta')^{\to v}\|_q^q \right) \\
&+ \sum_{v \in N_{\text{out}} \setminus N_{\text{in}}} \|\theta^{\to v}\|_q^q \max_{p \in \mathcal{P}^{\to v}} \sum_{\ell=1}^{\mathtt{length}(p)-1} \left(|b_{p_\ell} - b'_{p_\ell}|^q + \|\theta^{\to p_\ell} - (\theta')^{\to p_\ell}\|_q^q \right) \\
&\leqslant \sum_{v \in N_{\text{out}} \setminus N_{\text{in}}} \left(|b_v - b'_v|^q + \|\theta^{\to v} - (\theta')^{\to v}\|_q^q \right) \\
&+ \left(\sum_{v \in N_{\text{out}} \setminus N_{\text{in}}} \|\theta^{\to v}\|_q^q \right) \max_{p \in \mathcal{P} : p_{\text{end}} \notin N_{\text{in}}} \sum_{\ell=1}^{\mathtt{length}(p)-1} \left(|b_{p_\ell} - b'_{p_\ell}|^q + \|\theta^{\to p_\ell} - (\theta')^{\to p_\ell}\|_q^q \right).
\end{aligned}$$

It remains to use that $\sum_{v\in N_{\text{out}}\setminus N_{\text{in}}} \|\theta^{\to u_v}\|_q^q \leqslant \|\Phi(\theta)\|_q^q$ for normalized parameters θ [Gonon et al., 2024, Theorem B.1, case of equality] to conclude that:

$$\|\Phi(\theta)-\Phi(\theta')\|_q^q \leqslant \sum_{v\in N_{\text{out}}\setminus N_{\text{in}}} \left(|b_v - b'_v|^q + \|\theta^{\to v} - (\theta')^{\to v}\|_q^q\right) + \boldsymbol{\|\Phi(\theta)\|_q^q} \max_{p\in\mathcal{P}:p_{\text{end}}\notin N_{\text{in}}} \sum_{\ell=1}^{\texttt{length}(p)-1} \left(|b_{p_\ell} - b'_{p_\ell}|^q + \|\theta^{\to p_\ell} - (\theta')^{\to p_\ell}\|_q^q\right).$$

The term in **blue** can be replaced by $\boldsymbol{\min\left(\|\Phi(\theta)\|_q^q, \|\Phi(\theta')\|_q^q\right)}$ by repeating the proof with θ and θ' exchanged (everything else is invariant under this exchange). □

Lemma F.3. *Consider a DAG ReLU network with $L := D-1$ where the depth D is $\max_{path\ p\in\mathcal{P}} |\texttt{length}(p)|$ and width $W = \max(d_{out}, \max_{neuron\ v\in N} |\operatorname{ant}(v)|)$ where $\operatorname{ant}(v)$ is the set of antecedents of v in the DAG. Denote by θ the normalized parameters of θ as obtained as the output of Algorithm 1 in Gonon et al. [2024] with $q=1$, i.e., θ is obtained from θ by rescaling neurons from the input to output layer, ensuring every neuron has a vector of incoming weights equal to one on all layers except the last one. It holds for every θ,θ' and every $q\in[1,\infty)$*

$$\|\Phi(\theta)-\Phi(\theta')\|_q^q \leqslant (W^2 + \min(\|\Phi(\theta)\|_q^q, \|\Phi(\theta')\|_q^q)\cdot LW)\|\theta-\theta'\|_\infty^q$$

Lemma 3.3 corresponds to Lemma F.3 with $q=1$.

Proof of Lemma F.3. Lemma B.1 of Gonon et al. [2024] guarantees that $\Phi(\mathtt{N}(\theta)) = \Phi(\theta)$ for every θ. In particular,

$$\|\Phi(\theta)-\Phi(\theta')\|_1 = \|\Phi(\mathtt{N}(\theta)) - \Phi(\mathtt{N}(\theta'))\|_1$$

so it is enough to prove Lemma F.3 for *normalized* parameters, so we may and will assume $\theta = \mathtt{N}(\theta), \theta' = \mathtt{N}(\theta')$. Denote $\bar\theta^{\to v} := (\theta^{\to v}, b_v)$. With this notation, (23) implies (for normalized parameters θ,θ')

$$\begin{aligned}
\|\Phi(\theta)-\Phi(\theta')\|_q^q &\leqslant \sum_{v\in N_{\text{out}}\setminus N_{\text{in}}} \|\bar\theta^{\to v} - (\bar\theta')^{\to v}\|_q^q + \min(\|\Phi(\theta)\|_q^q, \|\Phi(\theta')\|_q^q)\cdot \max_{p\in\mathcal{P}:p_{\text{end}}\notin N_{\text{in}}} \sum_{\ell=1}^{\texttt{length}(p)-1} \|\bar\theta^{\to p_\ell} - (\bar\theta')^{\to p_\ell}\|_q^q \\
&\leqslant \sum_{v\in N_{\text{out}}\setminus N_{\text{in}}} |\operatorname{ant}(v)|\cdot\|\bar\theta^{\to v} - (\bar\theta')^{\to v}\|_\infty^q \\
&\quad + \min(\|\Phi(\theta)\|_q^q, \|\Phi(\theta')\|_q^q)\cdot \max_{p\in\mathcal{P}:p_{\text{end}}\notin N_{\text{in}}} \sum_{\ell=1}^{\texttt{length}(p)-1} |\operatorname{ant}(p_\ell)|\cdot\|\bar\theta^{\to p_\ell} - (\bar\theta')^{\to p_\ell}\|_\infty^q \\
&\leqslant \left(\sum_{v\in N_{\text{out}}\setminus N_{\text{in}}} |\operatorname{ant}(v)| + \min(\|\Phi(\theta)\|_q^q, \|\Phi(\theta')\|_q^q)\cdot \max_{p\in\mathcal{P}:p_{\text{end}}\notin N_{\text{in}}} \left(\sum_{\ell=1}^{\texttt{length}(p)-1} |\operatorname{ant}(p_\ell)|\right)\right)\|\theta-\theta'\|_\infty^q
\end{aligned}$$

The maximum length of a path is $D = L+1$. Moreover $W \geqslant d_{\text{out}} = |N_{\text{out}}|$ and $W \geqslant |\operatorname{ant}(v)|$ for every neuron, so this yields

$$\|\Phi(\theta)-\Phi(\theta')\|_q^q \leqslant (W^2 + \min(\|\Phi(\theta)\|_q^q, \|\Phi(\theta')\|_q^q)\cdot LW)\|\theta-\theta'\|_\infty.$$

□

G Recovering a known bound with Theorem 3.1

It is already known in the literature that for every input x and every parameters θ,θ' (even with different signs) of a layered fully-connected neural network with L affine layers and $L+1$ layers of neurons, $N_0 = N_{\text{in}}, \dots, N_L = N_{\text{out}}$, width $W := \max_{0\leqslant\ell\leqslant L}|N_\ell|$, and each matrix having some operator norm bounded by

$R \geqslant 1$, it holds [Gonon et al., 2023, Theorem III.1 with $p = q = \infty$ and $D = \|x\|_\infty$][Berner et al., 2020, Neyshabur et al., 2018]:

$$\|R_\theta(x) - R_{\theta'}(x)\|_1 \leqslant (W\|x\|_\infty + 1)WL^2R^{L-1}\|\theta - \theta'\|_\infty.$$

Can it be retrieved from Theorem 3.1? Next corollary almost recovers it: with $W\max(\|x\|_\infty, 1)$ instead of $W\|x\|_\infty + 1$, and $2L$ instead of L^2. This is better as soon as there are at least $L \geqslant 2$ layers and as soon as the input satisfies $\|x\|_\infty \geqslant 1$.

Corollary G.1. *[Gonon et al., 2023, Theorem III.1] Consider a simple layered fully-connected neural network architecture with $L \geqslant 1$ layers, corresponding to functions $R_\theta(x) = M_L\,\mathrm{ReLU}(M_{L-1}\dots\mathrm{ReLU}(M_1x))$ with each M_ℓ denoting a matrix, and parameters $\theta = (M_1, \dots, M_L)$. For a matrix M, denote by $\|M\|_{1,\infty}$ the maximum ℓ^1 norm of a row of M. Consider $R \geqslant 1$ and define the set Θ of parameters $\theta = (M_1, \dots, M_L)$ such that $\|M_\ell\|_{1,\infty} \leqslant R$ for every $\ell \in [\![1, L]\!]$. Then, for every parameters $\theta, \theta' \in \Theta$, and every input x:*

$$\|R_\theta(x) - R_{\theta'}(x)\|_1 \leqslant \max(\|x\|_\infty, 1)2LW^2R^{L-1}\|\theta - \theta'\|_\infty.$$

Proof. For every neuron v, define $f(v) := \ell$ such that neuron v belongs to the output neurons of matrix M_ℓ (i.e., of layer ℓ). By Lemma F.1 with $q = 1$, we have for every neuron v

$$\begin{aligned}
&\|\Phi^{\to v}(\theta) - \Phi^{\to v}(\theta')\|_1 \\
&\leqslant \max_{p\in\mathcal{P}^{\to v}} \sum_{\ell=1}^{\mathtt{length}(p)} \left(\prod_{k=\ell+1}^{\mathtt{length}(p)} \underbrace{\|\theta^{\to p_k}\|_1}_{\substack{\leqslant \|M_{f(p_k)}\|_{1,\infty} \\ \leqslant R}} \right) \\
&\qquad \left(\underbrace{|b_{p_\ell} - b'_{p_\ell}|}_{=0 \text{ (no biases)}} + \underbrace{\|\theta^{\to p_\ell} - (\theta')^{\to p_\ell}\|_1}_{\leqslant |\operatorname{ant}(p_\ell)|\|\theta-\theta'\|_\infty \leqslant W\|\theta-\theta'\|_\infty} \max_{u\in\operatorname{ant}(p_\ell)} \|\Phi^{\to u}(\theta')\|_1 \right) \qquad (24) \\
&\leqslant W\|\theta - \theta'\|_\infty \max_{p\in\mathcal{P}^{\to v}} \sum_{\ell=1}^{\mathtt{length}(p)} R^{\mathtt{length}(p)-\ell} \max_{u\in\operatorname{ant}(p_\ell)} \|\Phi^{\to u}(\theta')\|_1 \qquad (25)
\end{aligned}$$

with the convention that an empty sum and product are respectively equal to zero and one. Consider $\theta' = 0$. It holds $\|\Phi^{\to u}(\theta')\|_1 = 0$ for every $u \notin N_{\text{in}}$, and $\|\Phi^{\to u}(\theta')\|_1 = 1$ for input neurons u (Definition A.5). Therefore, we have:

$$\max_{u\in\operatorname{ant}(p_\ell)} \|\Phi^{\to u}(\theta')\|_1 = \mathbb{1}_{\operatorname{ant}(p_\ell)\cap N_{\text{in}}\neq\emptyset} = \mathbb{1}_{\ell=1 \text{ and } p_0\in N_{\text{in}}}. \qquad (26)$$

Specializing Inequality (24) to $\theta' = 0$ and using Equation (26) yields

$$\begin{aligned}
\|\Phi^{\to v}(\theta)\|_1 &\leqslant \max_{p\in\mathcal{P}^{\to v}} \sum_{\ell=1}^{\mathtt{length}(p)} \left(\prod_{k=\ell+1}^{\mathtt{length}(p)} R \right) \underbrace{\|\theta^{\to p_\ell}\|_1}_{\substack{\leqslant \|M_{f(p_\ell)}\|_{1,\infty} \\ \leqslant R}} \underbrace{\max_{u\in\operatorname{ant}(p_\ell)} \|\Phi^{\to u}(\theta')\|_1}_{=\mathbb{1}_{\ell=1 \text{ and } p_0\in N_{\text{in}}}} \\
&= \max_{p\in\mathcal{P}^{\to v}: p_0\in N_{\text{in}}} R^{\mathtt{length}(p)}. \qquad (27)
\end{aligned}$$

Since the network is layered, every neuron $u \in \operatorname{ant}(p_\ell)$ is on the $\ell - 1$-th layer, and every $p' \in \mathcal{P}^{\to u}$ is of

length $\ell - 1$, hence we deduce using Inequality (25), Equation (27) for θ' and u:

$$\begin{aligned}
\|\Phi^{\to v}(\theta) - \Phi^{\to v}(\theta')\|_1 &\leqslant W\|\theta - \theta'\|_\infty \max_{p \in \mathcal{P}^{\to v}} \sum_{\ell=1}^{\texttt{length}(p)} R^{\texttt{length}(p)-\ell} \underbrace{\max_{u \in \text{ant}(p_\ell)} \max_{p' \in \mathcal{P}^{\to u} : p'_0 \in N_{\text{in}}} R^{\texttt{length}(p')}}_{=R^{\ell-1}} \\
&= W\|\theta - \theta'\|_\infty \max_{p \in \mathcal{P}^{\to v}} \underbrace{\sum_{\ell=1}^{\texttt{length}(p)} R^{\texttt{length}(p)-1}}_{\leqslant LR^{L-1}} \\
&\leqslant LWR^{L-1}\|\theta - \theta'\|_\infty.
\end{aligned}$$

We get:

$$\begin{aligned}
\|\Phi(\theta) - \Phi(\theta')\|_1 &= \sum_{v \in N_{\text{out}} \setminus N_{\text{in}}} \|\Phi^{\to v}(\theta) - \Phi^{\to v}(\theta')\|_1 \\
&\leqslant |N_{\text{out}} \setminus N_{\text{in}}| \cdot LWR^{L-1}\|\theta - \theta'\|_\infty \\
&\leqslant LW^2R^{L-1}\|\theta - \theta'\|_\infty. \qquad (28)
\end{aligned}$$

Using Corollary B.2 with $q = 1$, we deduce that as soon as θ, θ' satisfy $\theta_i\theta'_i \geqslant 0$ for every parameter coordinate i, then for every input x:

$$\|R_\theta(x) - R_{\theta'}(x)\|_1 \leqslant \max(\|x\|_\infty, 1)LW^2R^{L-1}\|\theta - \theta'\|_\infty. \qquad (29)$$

Now, consider general parameters θ and θ'. Define θ^{inter} to be such that for every parameter coordinate i:

$$\theta_i^{\text{inter}} = \begin{cases} \theta'_i & \text{if } \theta_i\theta'_i \geqslant 0, \\ 0 & \text{otherwise.} \end{cases}$$

By definition, it holds for every parameter coordinate i: $\theta_i^{\text{inter}}\theta_i \geqslant 0$ and $\theta_i^{\text{inter}}\theta'_i \geqslant 0$ so we can apply Inequality (29) to the pairs $(\theta, \theta^{\text{inter}})$ and $(\theta^{\text{inter}}, \theta')$ to get:

$$\begin{aligned}
\|R_\theta(x) - R_{\theta'}(x)\|_1 &\leqslant \|R_\theta(x) - R_{\theta^{\text{inter}}}(x)\|_1 + \|R_{\theta^{\text{inter}}}(x) - R_{\theta'}(x)\|_1 \\
&\leqslant \max(\|x\|_\infty, 1)LW^2R^{L-1}\left(\|\theta - \theta^{\text{inter}}\|_\infty + \|\theta^{\text{inter}} - \theta'\|_\infty\right).
\end{aligned}$$

It remains to see that $\|\theta - \theta^{\text{inter}}\|_\infty + \|\theta^{\text{inter}} - \theta'\|_\infty = 2\|\theta - \theta'\|_\infty$. Consider a parameter coordinate i.

If $\theta_i\theta'_i \geqslant 0$ then $\theta_i^{\text{inter}} = \theta'_i$ and:

$$|\theta_i - \theta'_i| = |\theta_i - \theta_i^{\text{inter}}| + |\theta_i^{\text{inter}} - \theta'_i|.$$

Otherwise, $\theta_i^{\text{inter}} = 0$ and:

$$\begin{aligned}
|\theta_i - \theta'_i| &= |\theta_i| + |\theta'_i| \\
&= |\theta_i - \theta_i^{\text{inter}}| + |\theta_i^{\text{inter}} - \theta'_i|.
\end{aligned}$$

This implies $\|\theta - \theta^{\text{inter}}\|_\infty = \max_i |\theta_i - \theta_i^{\text{inter}}| \leqslant \max_i |\theta_i - \theta_i^{\text{inter}}| + |\theta_i^{\text{inter}} - \theta'_i| = \|\theta - \theta'\|_\infty$ and similarly $\|\theta^{\text{inter}} - \theta'\|_\infty \leqslant \|\theta - \theta'\|_\infty$. This yields the desired result:

$$\|R_\theta(x) - R_{\theta'}(x)\|_1 \leqslant \max(\|x\|_\infty, 1)2LW^2R^{L-1}\|\theta - \theta'\|_\infty. \qquad \square$$